ARGENTINE REPUBLIC
INTERIM REPORT ON THE NORTHERN NEUQUEN GEOTHERMAL DEVELOPMENT PROJECT

FIRST·SECOND PHASE SURVEY

NOVEMBER 1983

JAPAN INTERNATIONAL COOPERATION AGENCY

Contents

List of Figures

Foreword

This is an interim report on the 1st phase and 2nd phase surveys of the "Northern Neuquen Geothermal Development Project" carried out in compliance with the S/W (Scope of Work) signed February 25th 1982 between the Government of Japan and the Government of the Argentine Republic and on the analysis and discussion of data and information obtained by the said surveys.

During the execution of these surveys the survey team got an extremely positive and friendly cooperation of the counterparts of the Argentine Government and Province of Neuquén, in addition to a valuable support of the local Japanese diplomatic establishments. The survey progressed satisfactorily and we succeeded at obtaining very interesting data and samples both in the 1st and 2nd phases. As a consequence of the analysis and discussion of the said data and samples we succeeded at narrowing down gradually the target in the northern region of the Province of Neuquén by using methods of various kinds described in this interim report. We came to the conclusion that an area of approximately 40 Km^2 in the Domuyo district is extremely promising as a place of occurrence of geothermal energy storage area. Such being the case, we regard it indispensable to carry out the next stage of survey in order to investigate in further details and confirm the existence of the said geothermal energy storage structure.

In presenting this interim report the members of the survey team wish to express their best gratitude to the cooperation and support of the Argentine and Japanese organizations related to the matter and to the people of the survey areas.

Summary

1. The survey in question concerned with geothermal energy resources and covering an area of 15,000 square kilometers in the northern part of the Province of Neuquén, Argentine Republic, started in February 1982 and was carried out in 3 distinct phases ranging from the regional survey to the detailed survey by using various methods of investigation. This survey has two principal purposes, i.e., to make the final selection of the most promising area containing geothermal energy storage layer, with elucidation, comprehension and evaluation of the structure of the said layer, and to propose an appropriate course and plan about the investigations to be carried out in the future, including considerations about drilling of investigation wells and other details regarded as necessary.

2. The regional reconnaissance survey of the first phase (first survey), covering an area of 15,000 Km^2 including places with indications of geothermal energy, i.e., Vn. Domuyo, Vn. Tromen and Co. Carrere and consisting of remote sensing analysis, aerial photograph geological analysis and ground survey was carried out in February and March of 1982. After identifying and confirming the regional geological structure and the state of things of each site with geothermal manifestations, the Domuyo geothermal area with extension of 200 Km^2 and located at the west side of Vn. Domuyo was selected as most promising site to be taken into consideration as object of further detailed investigation in the second phase survey.

3. The second phase survey (second survey) covering an extension of 200 Km^2 of the Domu Domuyo area and consisting of detailed investigations through geological, geochemical, hydrological and gravity methods was carried out from November 1982 to March 1983. The potentiality of the site and the necessity of the next stage of survey were confirmed and the most promising priority area to be taken into consideration as object of the third phase survey was narrowed down to 40 Km^2.

4. High-temperature and conspicuous indications of geothermy accompanied with gushing out of hot spring, steam and gas are observed very frequently in the Domuyo area. Furthermore, extremely promising and interesting information about the following aspects were obtained as a result of the survey.

(1) Geological structure through data related to the geological stratigraphy, gravity anomalies, fault/fracture systems, etc.

(2) Geothermal structure and geothermal fluid structure through geochemical data and hydrological data such as soil, hot spring, steam, gas, etc.

(3) Geothermal reservoir structure through data obtained by comprehensive analysis of the aforestated information, etc.

5. A final and comprehensive analysis and discussion to be carried out concurrently with investigations of various kinds consisting principally of the undermentioned items are required in the third phase survey to be implemented futurely, in order to obtain information about great subterranean depths in the most promising extent of 40 Km^2 selected as a results of the surveys carried out so far, for the sake of identifying in details the underground structure and the geothermal fluid structure and to evaluate the potential of the site.

(1) Detailed investigation of the stratigraphic basement structure and fault system through seismic reflection method.

(2) Investigation of alteration zones and low specific resistance zones at great subterranean depths through vertical electrical prospecting.

(3) Investigation of underground thermal flow through thermometric survey in boreholes.

1. General Remarks

1. General Remarks

1.1 Purposes and Methods of Survey

This survey was started in accordance with the S/W (Scope of Work) signed February 25th 1982, based on the agreement between the Japanese Government and the Argentine Republic Government. The aforementioned S/W was signed by the duly authorized persons of the following organizations related to the matter.

From the Japanese side:

- Japan International Cooperation Agency (JICA)

From the Argentine side:

- Planning Coordination Undersecretariat, Planning Secretariat of the President of the Nation
- Subsecretariat of Fuels Resources of the State Energy Secretariat
- Secretariat del COPADE, Government of the Neuquén's Province

The survey in question, concerned with geothermal energy resources and covering an area of 15,000 Km^2 in the northern part of the Province of Neuquén, Argentine Republic, was carried out in three distinct phases ranging from the regional survey to the detailed survey by using various methods of investigation has two principal purposes, i.e., to make the final selection of the most promising area containing geothermal energy storage structure, with elucidation, comprehension and evaluation of the structure of the said layer, and to propose an appropriate course and plan about the investigations to be carried out in the future, including considerations about drilling of investigation wells and other details regarded as necessary.

The area object of survey, the flow chart of the three-phase survey and the stages of execution of work are shown in the Fig. 1-1, Table 1-1 and Table 1-2.

1.2 Outline of the First Phase Survey (First Year)

The first phase survey (first year) was carried out in February and March of 1982. The target of the promising area for geothermal development was narrowed down to 200 Km^2 as a result of the interpretations of satellite (LANDSAT) images covering 15,000 Km^2 and earial photographs covering 5,000 Km^2 located in the northern part of the Province of Neuquén. That promising area was selected as object of the second phase survey (second year).

1.3 Outline of the Second Phase Survey (Second Year)

The second phase survey commenced with the topographical mapping of the survey area (200 Km^2) prior to the execution of the field survey. Later on, the field survey consisting of geological survey, petrographical survey and rock sample test, gravimetric survey, alteration zone survey, 1 m depth ground temperature survey, geochemical survey, hydrological survey, survey of hot springs and fumarolic gas and vapour was carried out from November 1982 to March 1983. The geology, geological structure, geothermal structure,

geothermal fluid circulation structure and the geothermal reservoir structure are elucidated by making a comprehensive analysis of the aforementioned surveys. Extremely promising and interesting information were obtained as a result of the aforestated studies. Such being the case, the priority promising area of 40 Km^2 to be investigated in the third phase survey (third year) is selected and the concrete measures for implementation of the survey are planned.

1.4 Members and Schedule of the Survey Team

The members of the Japanese survey team and Argentine counterparts and the survey schedule are as follows.

(1) Survey team of the first phase

Japanese team			Argentine team		
Post	Name	Belong to	Post	Name	Belong to
Leader	Mr. Kaneo KAKEGAWA	JICA	Leader	Mr. Alfredo ESTEVES	Gov. of Neuguen Prov.
Geology	Mr. Fukio KAYUKAWA	"	Geochemistry	Mr. Jose L. SIERRA	"
Remote sensing	Mr. Tokichiro TANI	"			

Survey period (Period of stay in Argentine)

February 25th 1982 to March 31st 1982

Field survey period

March 8th 1982 to March 20 1982

(2) Survey team of second phase

Japanese team			Argentine team		
Post	Name	Belong to	Post	Name	Belong to
Leader	Mr. Kaneo KAKEGAWA	JICA	Leader	Mr. Alfredo ESTEVES	Gov. of Neuguen prov.
Geology	Mr. Fukio KAYUKAWA	"	Geochemistry	Mr. Jose L. SIERRA	"
Geology	Mr. Osamu MIYAISHI	"	Geology	Mr. Mario O. GINGINS	"
Geochemistry	Mr. Hisanao KOIZUMI	"	Geology	Mr. Luis C. MAS	"
Geochemistry	Mr. Kazuyasu SUGAWARA	"	Geochemistry	Miss Miriam LOEWY	"
Geophysics	Mr. Kenichi NOMURA	"	Topography	Mr. Juan de D. ALBORNOZ	"
Geophysics	Mr. Shigeo MORIBAYASHI	"	Topography	Mr. Carlos R. FERNANDEZ	"
Geophysics	Mr. Ikuo TAKAHASHI	"			

Survey period (Period of stay in Argentine)

November 15th 1982 to March 31st 1983

Field survey period

December 9th 1982 to February 28th 1983

Period of analysis and interpretation

April 1st 1983 to August 10th 1983

1.5 Implementation of the Survey

The survey work carried out so far in the first phase and in the second phase are summarized in the Table 1-3.

Table 1-3 Specific survey work carried out by the survey team

Phase	Contents				Volume of work
First Phase	Interpretation of LANDSAT images (1:250,000 scale)				15,000 Km^2 (2 images)
	Interpretation of aerial photographs (1:50,000 scale)				1,200 Km^2 (150 sheets)
	Reconnaissance geological survey	Explored distance of regional survey			500 Km
		Explored distance in Domuyo area			150 Km
Second Phase	Preparation of topographic map (1:25,000 scale)				200 Km^2
	Geological survey	Surveyed area			200 Km^2
		Explored distance			315 Km
		Quantity of specimens	Thin section		110
			X-ray analysis		130
			Age dating		8
			Physical properties		60
		Measurement of discharges			28 points
	Geochemical prospecting	Temperature at 1 m depth Hg concentration in soil CO_2 concentration in Soil-air		Regional survey	460
				Detailed survey	57
				Total	517
		Hot spring samples			18
		Gas samples			9
		Condensed water sample			9
	Gravity prospecting	Leveling	By autolevel		85 points
			By theodolite		137 points
			By altimeter		94 points
			Total		316 points
		Gravity measurement			316 points
		Regional survey	Measuring points		31 points
			Surveyed distance		1,050 Km

Table 1-1 Flow chart of the survey in three phases

Stage	Survey area	Methodology	Contents of survey	Expected data
First phase (First year)	(First part) 15,000 km^2	. Bibliographic compilation and analysis . Interpretation of satellite (LANDSAT) Images Selection of 5,000 km^2 . Photogeological interpretation quick looking of 5,000 km^2 mapping of 1,200 km^2 . Reconnaissance geological survey (ground survey and investigation of geothermal manifestations)	. Identifications of geology, structure, volcanoes, distribution of geothermal manifestations, fracture system, fault zones, drainage textures, grade of relative porosity, use of the land, characteristics of the geothermal manifestations, accessibility and topography.	. Background of the magmatic and geothermal activity. . Water balance, hot water storage structure, geothermal manifestations and volcanoes. . Determination of the most promising and adequate area for geothermal development. . Estimation of the geothermal system.
	(Second part) 5,000 km^2			
Second phase (Second year)	200 km^2	Selection of 200 km^2 . Topographical mapping . Geological survey . Petrographical survey . Hydrological survey . Survey of alteration zones . Test of rock samples (density, porosity, magnetic susceptibility, X-ray analysis, microscopic analysis, age dating) . Geochemical survey (temperature at 1 m depth, Hg in soil, CO_2 in soil -air, hot spring, fumarolic gas) . Gravity survey	. Geological constitution, stratigraphy, geologic structure, fracture systems, surface discharges, runoff, estimation of the infiltration and its scheme, distribution, types and extension of the alteration zones. . Texture, composition, density, porosity, alteration, age, relation with temperature, Hg and CO_2. . Distribution of hot springs and fumaroles, tendency of distribution. . Flow, composition, temperature, pH and electrical conductivity of spring water. . Gravity, underground structure.	. Extension of the layers, stratigraphic relation, thickness, microscopic structures of the rocks. . Water balance, scheme of supply of water as geothermal conductor. . Geothermal and magmatic activity (heat source) in terms of absolute age, thermal history, geothermal system, magnitude and temperature of the reservoir, scheme of ascent of the hydrothermal fluids. . Structure of the deep underground. . Model of geothermal reservoir.
Third stage (Third year)	40 km^2	Selection of 40 km^2 . Geoelectrical prospecting (Schlumberger method) . Seismic prospecting (reflection method) . Thermal gradient wells (100 m) . Core & cuttings survey . Core test (density, porosity, magnetic susceptibility, electric resistivity, microscopy, X-Ray analysis, thermal conductivity, seismic wave propagation velocity)	. Electric resistivity, deep structure . Elastic wave propagation velocity (P waves) . Thermal gradient, temperature distribution, electrical resistivity, spontaneous potential . Distribution and spacial variation of the rock density, porosity, resistivity, magnetic susceptibility, alteration, thermal conductivity and seismic wave propagation velocity.	. Extension, depth and form of low electric resistivity zones, geothermal structure. . Underground structure, extension, depth and form of low-velocity layers, temperature of heat sources, estimation of heat dispersion, underground temperature distribution and gradient, geothermal system, variation of the rock texture. . Model of geothermal reservoir (from the geothermal reservoir engineering standpoint). Evaluation of geothermal potential Proposition of the exploration well drilling program

Table 1-2 Schedule of the survey in 3 phases

Stage	Contents	1982												1983												1984											
		1	2	3	4	5	6	7	8	9	10	11	12	1	2	3	4	5	6	7	8	9	10	11	12	1	2	3	4	5	6	7	8	9	10	11	12
	Japanese fiscal year	← 1981 →						← 1982 →						← 1983 →												← 1984 →											
	Field survey (Possible)	▬	▬	▬	▬							▬	▬	▬	▬	▬	▬							▬	▬	▬	▬	▬	▬								
First phase (15,000km^2) Concluded	Previous preparations	⊢⊣																																			
	Satellite (LANDSAT) image interpretation (15,000km^2)	▬	▬	▬	▬																																
	Aerial photograph interpretation (5,000km^2)		▬	▬	▬																																
	Bibliographical compilation and analysis	▬	▬		▬	▭																															
	Geological survey			▬	▬	▬	▭																															
Second phase (200km^2) Concluded	Topographical mapping (200km^2)						▭	▭	▭	▭	▭																											
	Geological survey (200km^2)											▬	▬	▬	▬	▬	▬	▭	▭																			
	Test of rock samples													▬	▬	▬	▬	▭																			
	Hydrological survey											▬	▬	▬	▬	▬	▬	▭	▭																			
	Geochemical survey													▬	▬	▬	▬	▭	▭																			
	Survey of hot springs and fumarolic gases															▬	▬	▭																			
	Gravity survey (200km^2)													▬	▬	▬	▬	▭	▭																			
	Preparation of the manuscript of the report																	△	⊢⊣	△																		
Third phase (40km^2) Scheduled	Geoelectrical prospecting																										▬	▬	▬	▬	▭	▭						
	Seismic prospecting																										▬	▬	▬	▬	▭	▭						
	Drilling of 100m thermal gradient wells (supervision)																							▬	▬	▬	▬	▬	▬	▭	▭						
	Logging of 100m thermal gradient well																							▬	▬	▬	▬	▬	▬	▭	▭						
	Core test, analysis, etc.																										▬	▬	▬	▬	▭	▭					
	Preparation of Manuscript of report																														△	⊢⊣	△				
	Previous preparation and planning	▬	▭								▬	▭											▬	▭													
	Presentation of the preliminary report			△	⊢⊣	△									△	⊢⊣	△											△	⊢⊣	△							
	Discussion of the interim report manuscript																	▬	▭																		
	Discussion of the final report manuscript																															▭	▬	▭			
	Presentation of the report (JICA)																		⊢	-	-	▭												⊢	-	-	▭

2. Outlines of the First Phase Survey

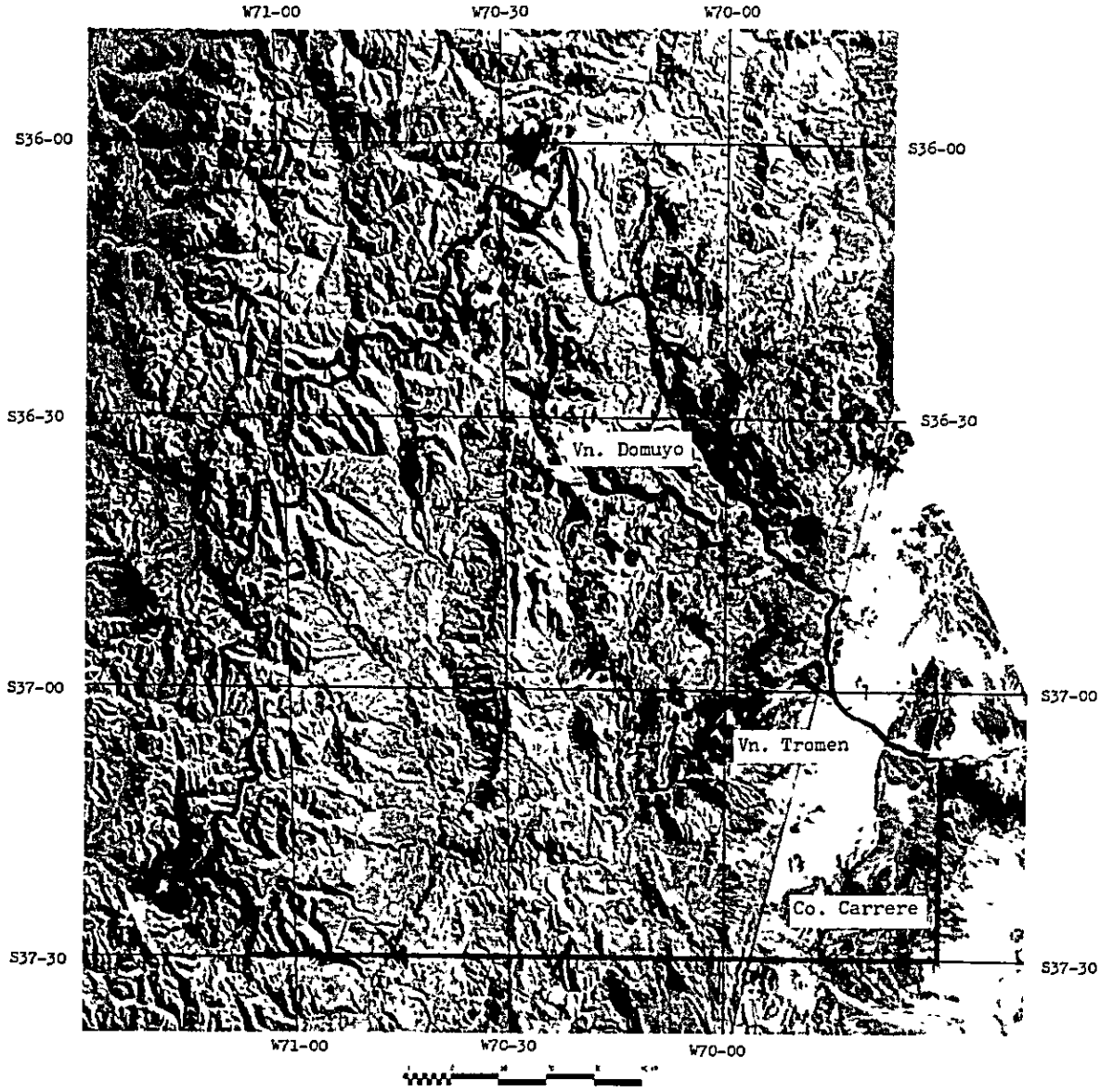

Plate 1 Landsat image of Vn. Domuyo area

2. Outlines of the First Phase Survey

2.1 Contents of the First Phase Regional Survey

The first phase regional survey corresponds to the first step of the three-year program for geothermal energy development surveys in the Province of Neuquén, Republic of Argentine.

Aiming to extract and select a promising area of about 200 Km^2 for the second phase survey, the following surveys were done in a preliminary investigation area covering approximately 15,000 Km^2 in the northern part of the Province.

(1) Analysis of Landsat image

Analyses of three scenes of Landsat image (Path 248 · Row 86, Path 249 · Row 86 and Path 249 · Row 85), covering the whole object area of about 15,000 Km^2, were conducted in Japan before field surveys.

The analytical method for three scenes of false color composite image in a scale of 1:250,000 is photogeologically to make out distributions and relations of geological units, such as basement rocks of Paleozoic and Mesozoic formations, Tertiary formation and younger volcanic rocks of Quaternary age. Keeping place with these analyses, principal tectonic lines were studied geologically.

By collation these results with available geological data, outlines of regional geology and geologic structure were compiled (Fig. 2-1).

(2) Photo-geological interpretation

Photo-geological interpretations for the area of 5,000 Km^2, which had been selected by studies of the analysis of Landsat image as well as regional geological map (Fig. 2-2), were done through the period of field surveys. The aerial photographs in a scale of 1:50,000 were available in Argentine, and their composite photographs were used for this study.

Because the object area of photogeological interpretation covers a wide area, a method of "Quick looking" by observations of composite and/or unit aerial photographs were employed for the greater part of object area except areas considered to be promising. These studies resulted in the assistance of analyses of Landsat image.

For the promising areas, drawings of detailed drainage map and detailed geological interpretations were conducted by a three-dimentional observation of aerial photographs.

As a result of these studies combined with results of a reconnaissance geological survey, geology and geologic structure as well as geothermal manifestation in the object area for the second phase survey were clarified. The area includes western parts of the Domuyo Volcano and those surrounding areas (Fig. 2-3).

(3) Reconnaissance geological survey

Based on analyses of Landsat image and photogeological interpretations combined with studies of available geological data, following three routes of reconnaissance geological

survey were selected, where younger volcanos such as Domuyo Volcano, Mt. Cruzada, Tromen Valcano and Mt. Carrere are located in the Cordillera del Vient, and geothermal manifestations related to younger volcanos are known.

1) Route along the Neuquén and Varvarco Rivers from Chos Malal through Andacallo, Las Ovejas and Varvarco to geothermal manifestation areas located at western parts of Domuyo Volcano.

2) Route from Chos Malal through Chapua to Tromen Volcano.

3) Route from Chos Malal through Chacayco and Auquinco to El Tril located north of Mt. Carreere.

2.2 Regional Geology and Geologic Structure

2.2.1 Outlines of Geology

(1) Stratigraphic sequence

Basement rocks in the region consist of sedimentary rocks and volcanic – pyroclastic rocks, which have been placed in the Permian and/or Triassic Time, and of plutonic rocks intruded into older formations.

Mesozoic formations, mainly consisting of sedimentary and pyroclastic rocks unconformably overlie the basement rocks.

Andestic volcanic activity occurred in the Tertiary age, and followed by related plutonic activity. At the end of the Tertiary age, acidic volcanic activity consisting of lava flows and pyroclastic rocks took place covering the basement rocks of Paleozoic and/or Mesozoic formations, and large-scale intrusive bodies of quartz porphyry and others were formed in the area centering around Domuyo Volcano. These rocks of acidic activity, in the lump, are called the Domuyo Volcano Complex.

At Quaternary time, younger volcanism of intermediate to acidic took place in this region and yielded lava flows of basaltic andesite, andesite, dacite and rhyolite.

(2) Basement rocks and Mesozoic formation

Choiyoi Group of the basement, considering to be Permo-Triassic System, is represented by well stratified mudstone interbedded with sandstone and limestone occasionally with intercolations of basalt or propylite lavas, along areas of the routes from Chos Malal, to Varvarco, Tromen Volcano and El Tril.

Along the route from Varvarco to Domuyo, rhyolitic lava flows and their pyroclastic rocks dominate the Group and are intruded by diorite, granodiorite and fine-grained granite.

Mesozoic formations are divided into Chacay Melehue Formation, Auquilco Formation, Tordillo Formation and Mendoza Group in ascending order. Chacay Melehue Formation unconformably covers Choiyoi Group. It is composed of breccias constituting by dominant

rhyolitic fragments and sandy or tuffaceous matrix in the lower part, and of white-grey sandstone, black mudstone and dark colored marl in the upper part. Auquilco Formation conformably overlies Chacay Melehue Formation, and consists of beds of limestone, sandstone and evaporite gypsum from lower to upper parts. Tordillo Formation succeeds Auquilco Formation and mainly consists of sandstone, which increases limonite in proportion to the upper part. Mudstone is predominant in the Mendoza Group.

(3) Tertiary formations and Domuyo Volcano Complex

Tertiary formations are divided into following three units. Namely, Pelan Formation is composed of andesite, andesite-porphyry, diorite-porphyry and fine-grained quartz diorite. Charilehue Formation consists of lava flows of andesite or basaltic andesite together with their pyroclastic rocks. Palao Granite is a stock-type intrusive body into Mendoza Group and forms Mt. Palao. Each Tertiary formations are believed to be Miocene in age.

Domuyo Valcano Complex can be divided into effusive facies and intrusive facies. The former consists of alternating beds of rhyolitic tuff, lapilli tuff and tuff breccia, and of lave flows of rhyolite and dacite. It distributes at the western slope of Domuyo Volcano. The later forms stocks-shaped intrusive bodies centering around Domuyo Volcano and crops out in an area of approximately 24 Km^2. The lithology of the intrusive facies ranges from rhyolite-porphyry to granodiorite-porphyry, and shows felsitic lithology in case of dikes.

The activity of Domuyo Volcano Complex is considered to range from middle Miocene to early Pliocene in age.

(4) Volcanic rocks of late Tertiary to Quaternary

A sequence of volcanism took place in the region, and forms formations of lava flow and pyroclastic rock of basaltic andesite, andesite and decite. They are divided into Sierra de Flores Formation, Atreuco Formation, Ponchehue Formation and Celletas Formation. The latest volcanism in the region is Domo Volcanic Rocks distributed at the southwestern slope of Mt. Domuyo. They are composed of rhyolitic lava flows and pyroclastic rocks, and an absolute age of 0.72 ± 0.10 Ma is obtained from one of lava flows at the rather early stage which form Mt. Domo.

2.2.2 Outlines of Geologic Structure

Regional geologic structure, as shown in Fig. 2-2, is characterized by the fold structure trending in approximately N-S direction and plunging toward the north. As is mentioned in the later chapter, the areas of high gravity anomaly are entirely identical with those of anticlinal structure where basement rocks and Mesozoic formation are distributed. On the other hand, the areas of low gravity anomaly completely correspond to those of synclinal structure where cenozoic volcanic rocks are dominant. In addition, values of Bouguer anomaly have a tendency to decrease toward the north. This proves fold axes plunging toward north, structurely.

In the area of Domuyo Volcano, box-shaped dome structure has been formed centering

around Domuyo anticlinal axis of N-S direction. This dome-shaped upheaval block is composed of Choiyoi Group of basement, Chacay Melehue Formation, Auquilco Formation, Tordillo Formation and Mendoza Group of Mesozoic succeeding from center to outside. At the core of dome structure, intrusive rocks of Domuyo Volcano Complex are widely distributed.

Fault systems of N-S direction parallel to above-mentioned fold axes and of E-W direction are predominant in the region, accompanying with fault systems of NW-SE or WNW-ESE direction and of NE-SW or ENE-WSW direction.

As shown in Fig. 2-3, they can be made out as lineaments having various characteristics of strength and length by photogeological interpretations.

2.3 Regional Geothermal System

2.3.1 Outlines of Younger Volcano and Geothermal Manifestation

(1) Distributions of younger volcanos.

Younger volcanos such as Domuyo Volcano, Mt. La Cruzada, Tromen Volcano and Mt. Carrere are arranged in NW-SE direction in the mountain system of Cordillera del Viento. This volcanic activity was vigorous from latest Tertiary time through Quaternary in age, and erupted on the basement rocks of Paleozoic or Mesozoic formation. It is assumed that the volcanism was large-scale near areas of Domuyo Volcano in the northwestern part and it decreased near areas of Mt. Carrere in proportion to the southeastern part.

Outlines of volcanic activity of Domuyo Volcano were described before in connection with regional geology and geologic structure. In the area of Tromen Volcano, there are old and new volcanos. They hold their original shapes of volcano, and there is a dammed lake between two volcanos which was formed by basaltic lava flows. Volcanism of Tromen Volcano is supposed to be active up-to recent, however, volcano located at north of Tromen Volcano seems to be a little old.

Because volcanism formed Mt. Carrere is not to be large-scale, distributions of younger volcanic rock are limited.

(2) Distributions of geothermal manifestation

1) Domuyo Volcano and environs

Hot springs of El Turleio are 14 Km north of Domuyo Volcano, spring out from four points in flood plain of rivers which are located at western rims of distribution areas of Mendoza Group.

In the western and southwestern areas of Domuyo Volcano, there are the most predominant geothermal manifestations of hot springs and fumarolic gas. Namely, they are Rincon de Las Papas, El Humazo, Las Olletas, La Bramadora, Arroyo Aguas Calientes, Banos del Aguas Calientes and Los Tachos. All of them, except La Bramadora, spring out hot water and spout fumarolic gas from the uppermost part of beds of tuff breccia and overlying lava flows covering Mesozoic formations and/or basement rocks. At La Bramadora, fumarolic

gas spouts through fissures near boundary between intrusive rocks distributed near Domuyo Volcano and younger volcanic rocks.

Depositions of travertine and hydrothermal alteration zones can also be observed at areas of these geothermal manifestation.

2) Tromen Volcano and environs

In the areas of Tromen Volcano and another volcano located at north, no geothermal manifestation of hot spring or fumaloic gas is known. Although some underground water spring out, its temperature is as low as 8.5°C. Besides, there are only alteration zones without hot spring or fumaloic gas southwest of Tromen Volcano.

3) Northern area of Mt. Carrere

Agua Termal is known as a geothermal manifestation, where some underground water contained hydrogen sulphide spring out through fissures in mudstone of Paleozoic or Mesozoic formation. However, its temperature is as low as 20°C.

2.3.2 Preliminary Model of Geothermal System

Preliminary model of geothermal system in the western areas of Domuyo Volcano, where the most predominant geothermal manifestations of hot spring and fumaloic gas are distributed, is shown in Fig. 2-5. The model is composed by stratigraphic sequence, geologic structure, heat flow structure and circulation mechanism of goethermal fluid which are based on results of the first phase survey such as those of analyses of Landsat image, photogeological interpretations and reconnaissance geological survey together with studies of available data.

(1) Stratigraphically, the region is occupied by basement rocks of Paleozoic formation and intrusive bodies of granite, unconformably overlying Mesozoic formations, and Tertiary to Quaternary volcanic and pyroclastic rocks of various type. In the vicinity of Domuyo Volcano, younger volcanos of Quaternary age are located.

(2) Strong geothermal manifestation consisting of hot springs, fumaroles, travertines and hydrothermal alteration zones are widely distributed in the place of western part of Domuyo Volcano. It is assumed that a magma reservoir is latent at the depths of the region and is active as a heat source.

(3) Each of the rivers rising from Domuyo Volcano have running water through the whole year which is originated by glacier and eternal snow. There are necessary conditions that surface water permeates into subsurface and forms shallow and deep underground water, and that underground water becomes the source of hot spring water and deep geothermal hot water.

(4) Volcanic and pyroclastic rocks of Neogene Tertiary or Quaternary age range from compact lava flows to porous rocks like pumice-tuff. The parts of high permeability, caused to well developed fractures and/or porosity-rich beds, present places to form shallow hot water secondarily. However, it is supposed that younger volcanic formations may generally play important cap rocks for deep geothermal fluid reservoir.

(5) Younger volcanic formations have a remarkable unconformable relationship with underlying basement rocks or Mesozoic formations, and the basement is generally situated at the rather shallow depths. Underground water permeated into deep subsurface is heated by heat source and is result becomes deep geothermal hot water having its temperature of 200°C, to 250°C. The deep geothermal hot water forms deep geothermal fluid reservoir along and/or in fracture systems of faults and sheared zone developed in the basement rocks. Geothermal fluid consisting of deep geothermal hot water, steam and gas ascends through fracture systems from deep geothermal fluid reservoir. Then, it mixes with shallow ground water and makes a secondary shallow hot water reservoir having its temperature of 100°C or more along unconformable planes or among permeable strata. Furthermore, hot water, steam and gas ascend and finally reach the surface as geothernal outcrops of hot water and fumaloic gas.

2.4 Selection of Target Area for the Second Phase Survey and the Working Plan

2.4.1 Extraction of Target Area for the Second Phase Survey

Based on results of the first phase survey, the most promising area of approximately 200 Km^2 ranging 20 Km at E-W and 10 Km at N-S was selected among the whole object area for the second phase survey. This area covers drainage systems of Manchana Covunco, Aguas Calientes and Covunco Rivers between western part of Domuyo Volcano and eastern side of Varvarco River,and entierly includes many predominant geothermal manifestations such as Rincon de Las Papas, El Humazo, Las Olletas, La Bramadora, Arroyo Aguas Calientes, Banos del Aguas Calientes and Los Tachos.

2.4.2 Principle of the Second Phase Survey and the Proposed Working Plan

Assuming that above-mentioned preliminary model of geothermal system, principles of the second phase survey was set up as follows:

i) To make clear geology and geologic structure, heat flow structure, and circulation mechanism and reservoir structure of geothermal fluid,

ii) To make out more detailed model of geothermal system in the object area, based on results of the second phase survey,

and

iii) To set up principle and proposed working plan of the third phase survey.

On the basis of the above-mentioned principles, following detailed working plains were proposed to attain its purpose.

(1) Elusidation of geology and geologic structure

1) Preparation of topographic map

Detailed topographic maps which cover the whole object area, are required, in order to conduct various kinds of survey of the second phase. For this purpose, topographic maps of 1:25,000 in scale will be prepared by available aerial photographs.

2) Geological survey

Detailed geological survey will be carried out in order to make clear geological distribution and stratigraphic sequence, and to study histories on development of geologic structure and on volcanic activity.

The detailed geological survey will clarify relations between geothermal manifestations and volcanic activity, and characteristics of geothermal fluid reservoir and cap rock based on stratigraphic sequence and geologic structure.

3) Rock examination

Petrographic characteristics and physical properties of constituent rocks will be examined in order to make clear subsurface structure and to obtain basic data for geophysical prospecting. For this purpose, the following examinations will be carried out; absolute age, microscopic observation, chemical analysis and measurement physical properties of rocks.

4) Gravity prospecting

It is assumed that deep geothermal fluid reservoir and ascending paths of geothermal fluid have close relations with depth and form of basement rocks, and with fracture systems of fault and sheared zone developed in them.

Therefore, it is one of the most important studies to make clear factors of geologic structure, in order to extract promising target area for further geothermal energy development.

Based on results of the first phase survey, it was proved that there are differences of density between rocks of basement and rocks of overlying each formations and younger volcanic rocks. Accordingly, because gravity prospecting is considered to be very effective for the purpose of elusidation on subsurface structure, gravity prospecting will be conducted in the whole object area.

(2) Elusidation of heat flow structure

1) Alteration zone survey

Hydrothermal alteration as one of the geothermal manifestations gives a key to solve heat flow structure of subsurface and characteristics of deep geothermal fluid and hot water.

Therefore, distributions, characteristics and zoning of hydrothermal alteration will be studied together with geological survey and by X-ray diffraction analysis.

2) Ground temperature survey and geochemical prospecting

Ground temperature at 1 meter survey together with geochemical prospectings of Hg-concentration in soil and CO_2-concentration in soil-air will be carried out in the whole object area.

These survey and prospectings are useful methods for geothermal survey. Because, there are many cases that heat transmitted from the depths and Hg-CO_2 gas ascended through fracture systems reflect heat flow structure and circulation mechanism of geothermal fluid at the depths as anomalies on or near the surface.

(3) Elusidation of circulation mechanism of geothermal fluid

1) Hydrological survey

Meteorological and hydrological surveys in the object area will be conducted, in order to obtain basic data on water balance of surface and underground water which is one of the origins of geothermal fluid.

2) Geochemical survey of hot water, fumaloic gas and condensed water

Hot water and fumaloic gas are outcrops of geothermal phenomena. They give very important keys to make clear circulation mechanism of geothermal fluid, such as formation and origin of deep geothermal fluid, structure and condition of geothermal fluid reservoir, and circulation mechanism of deep geothermal fluid, hot water, underground water and surface water. Putting results of these geochemical anomalies, hydrothermal alteration zones and Hg-CO_2 concentration anomalies together, geothermal system in the object area will be studied in detail.

(4) Establishment of detailed model of geothermal system and plan of the third phase survey

Combined with all results of the first and second phase surveys, more detailed model of geothermal system will be studied. Furthermore, the most promising area will be selected as a target area for the third phase survey, and its principle and proposed working plan will be established.

3. Geology in the Investigation Area

3. Geology in the Investigation Area

3.1 Preparation of Topographic Map

Topographic maps in scale of 1:100,000 and 1:500,000 of the region including the investigation area are available.

However, more detailed topographic maps which cover the whole object area are necessary, in order to conduct geological survey, geochemical and gravity prospectings and others of the second phase survey. For this purpose, topographic map in a scale of 1:25,000 was prepared by using aerial photographs before field surveys.

The photographs used were offered by the Republic of Argentine. They had been taken by Direccion General de Fabricaciones Miliales in 1962 and 1963 for the Plan Cordillerano. Conditions of photographing are as follows;

Camera used: WILD RC8 (focal distance 152.4 mm)

Flight hight : 8,534 to 10,668 m

Scale of photographing : approximately 1:50,000

List of aerial photographs : shown in Table 3-1

Flight courses: shown in Fig. 3-1

Table 3-1 List of aerial photographs

Course No.	*Photograph Number*	*No. of sheets*
C-6	3,120 ~ 3,124	5
C-7	2,041 ~ 2,048	8
C-8B	3,208 ~ 3,212	5
C-8	2,159 ~ 2,163	5
C-9	2,263 ~ 2,265	3

Table 3-2 List of survey datum points

Code of point	Name of point	Gauss Krügger coordinates		Elevation (m)
		X	Y	
OH-I-22	Co. Butalon	5,918,036.25	2,361,335.70	2,982.00
OH-I-30	Cordillera Las Lloves	5,945,726.60	2,343,864.29	2,750.00
Datum level pt. 1	–	–	–	1,650.00
Datum level pt. 2	–	–	–	3,250.00
Datum level pt. 3	(Vn. Domuyo)	–	–	4,709.00

Because no triangulation station is available in the investigation area, X, Y cordinates and hights of two triangulation stations located outside of the area were used as standard points of drawing topographic maps. Besides, three bench marks, one in the area and two outside, were selected and used.

Fundamental topographic maps prepared are of a scale of 1:25,000, and enlarged maps in a scale of 1:10,000 and reduced maps in a scale of 50,000 are used for field surveys and for attached maps of this report, respectively. Fig. 3-2 shows a bird's-eye view map based on the topographic map.

As a result of surveyings during period of field surveys, arranging tentative standard points in the area, it was proved that there are some distortions in the map. This causes that two triangulation stations used for drawings are located at remote areas outside of the investigation area.

3.2 Stratigraphic Sequence and Geological Unit

Detailed geological survey was conducted in the western areas of Domuyo Volcano of approximately 200 Km^2 selected on the basis of results of the first phase survey. Total survey routes reached 315 Km, and more than 200 rock specimens were collected. Among them, each 110 and 8 specimens were supplied for thin sections and determinations of absolute age. In order to study geology of the investigation area in connection with regional geology, routes from the area to Andacollo south of the area were geologically inspected. In addition, regional geology between City of Neuquen and Dmuyo Volcano was observed from the air.

As a result of these studies, the investigation area is geologically divided into four units of basement rocks, Mesozoic formations, Tertiary formations and younger volcanic rocks taken place during late Tertiary to Quaternary time in ascenting order (Fig. 3-3, 3-4 and 3-5). Table 3-3 shows geological correlation table.

3.2.1 Basement Rocks

Basement rocks in the investigation area consist of metamorphic rocks of Choiyoi Group, which have been intruded into older formations.

Crystalline schists, pelitic shist and psammitic shist, are restricted in distribution at western part of Rincon de Las Papas. Their schistose planes strike N70°E and dip 45° ~ 60°NW.

Various kinds of hornfels crop out near El Humazo. They are consisting of dark colored hornfels originated from basic tuff and basic sandy tuff and of hornfels derived from sandstone and/or mudstone, and strike N40°W and dip 60°NE.

Varvarco Plutonic Rocks crop out along Varvarco River and Manchana Covunco River, beside they distribute at the western slope of Cerro de La Papa and near the Covunco River and Atreuco River. Lithology of the plutonic rocks is represented by medium to coarse-grained hornblende-biotite granodiorite. Pink-colored aplitic granite is also observed as small-

Table 3-3 Correlation table of stratigraphic sequence

Age			Zollner y Amos (1973) Descripción geologica de la Hoja 32b, Chos Malal	Llambias et al (1978)		Brousse y Besce (1982)		JICA (1983)	
				Formation	Lithology	Formation	Lithology	Formation	Lithology
Cenozoic	Quaternary	Holocene	Recent alluvium Basalt VII Basalt VI						Recent alluvium Reworked tuff Basalt lave
		Pleistocene	Basalt V Glacial deposit Gravel Basalt IV Basalt III Andesite III			Magmatismo Domico	Rhyolite		Rhyolite lava Dacite lava Perlite Dacitic tuff breccia
	Tertiary	Pliocene	Basalt II Basalt (uncertain)	Atreuco F.	Andesitic-basic andesitic lava	Atreuco F.	Latite		Andesitic tuff breccia Volcanic breccia
			Unconformity	Domuyo volcanic complex	Rhyolitic, dacitic and andesitic lava and breccia Tuff and Tuff breccia	Sierra de Flores F.	Andesite, basic andesite		
		Miocene	Basalt I Basalt O	Charileue F.	Andesite, Basic andesite	Acidic Pyroclastics	Pumice flow		Andesite lava
			Unconformity			?	?		Discontinuity
		Oligocene Eocene Paleocene	Andesite, Andesitic tuff, Basaltic andesite and Olivine basalt						Dacitic lava Dacitic tuff breccia
			Unconformity						Discontinuity
Mesozoic	Cretaceous	Maastrichtian Campanian Santonian Coniacian Turonian Cenomanian	Gravel-bearing red sandstone						
			Unconformity						
		Albian Aptian Barremian Hauterivian Valanginian Berriasian	Soft clayey sandstone with salt body						
			Gypsum-Dolomite Breccia and Conglomerate						
			Claystone, Sandstone						
			Claystone						
			Claystone Marlaceous Claystone			G. Mendoza	Limestone Calcareous mudstone		
	Jurassic	Malm: Tithonian							
		Malm: Kimmeridgian Oxfordian	Tuff, Tuffaceous sandstone and Sandstone	Tordillo F.	Red sandstone Siltstone	Tordillo F.	Sandstone Siltstone		Discontinuity
								Tordillo F.	Dacitic fine tuff, Tuffaceous sandstone, Mudstone
			Gypsum claystone, Schistose marl and Dolomitic marl	Auquilco F.	Gypsum, Sandstone, etc.	Auquilco F.	Gypsum Sandstone	Auquilco F.	Sandstone Limestone Gypsum
		Dogger: Callovian Bathonian Bajocian	Schitose claystone, Marl Tuff, Tuffaceous sandstone, Lava	Chacay Melehue F.	Sandstone Mudstone Marl Breccia	La Manga F.	Sandstone Mudstone Marl	Chacay Melehue F.	Mudstone, Andesitic tuff breccia, Andesitic lava, Lapilli tuff, Basaltic sandstone
			Unconformity						Discontinuity
		Lias	Claystone, Tuff, Reworked tuff, Conglomerate, Sandstone, Limestone and Schistose claystone						
			Unconformity						
	Triassic		Porphyrite and Quartz-porphyry	Choiyoi Group					Psammitic~pelitic hornfels, Basic hornfels, Pelitic~psammitic schist, Varvarco intrusive, Aplitic granite, Granodiorite
			Unconformity						
Paleozoic	Permian		Intrusion of granite and granodiorite						
	Carboniferous		Andesitic tuff breccia Shale and Siltstone Acidic tuff and Sandstone						

Plutonitas Varvarco

Granite Complex

scale dikes formed at the late stage of plutonism.

Although there is a hypothesis that plutonism of Varvarco instrusive rocks belongs to that of Cenozoic age, it can be regarded as intrusions during the period of late Permian to middle Jurassic age on a basic of results of age determination by K-Ar method, as described in the later chapter.

Silica rocks are observed as xenolith in granodiorite, and are pale green or green-colored, strongly silicified rocks which are difficult to assume their original rocks. Dikes of basalt intruded into granodiorite are of small-scale, and show dark-color by chloritization.

3.2.2 Mesozoic Formations

Mesozoic formation in the investigation area composed of Chacay Melehue, Auquilco and Tordillo Formations which are correlatable to the Dogger to Malm Series.

(1) Chacay Melehue Formation

Chacay Melehue Formation is mainly composed of beds of basaltic or andesitic tuff and tuff breccia, lava flows of basalt and andesite, and interbedded members of black shale. The estimated thickness is 1,000 meters.

Lithology of volcanic rocks of the Formation shows basaltic at lower portions and changes to andesitic, partially dacitic, at upper parts, and they are generally suffered by strong chloritization.

Two members of black shale are interbedded at the upper and upper-most parts of the Formation, and are of hardly consolidated and well stratified shale. Fossils, found in lower member of black shale interbedded in andesitic rocks, are of Sonnĩnia Sp. of ammonite and indicate the Bajocian stage of middle Jurassic, as a result of studies by Mining Bureau of the Province of Neuquén.

Chacay Melehue Formation distributes in areas from east of El Humazo to La Bramadora, and also occurs at areas near and west of Rincon de Las Papas and southern-most part of the investigation area. Because it strikes N-S and dips 20° ~ 30°E at least of El Humazo and dips 30° ~ 40°NW at La Bramadora, an existence of synclinal structure is assumed between two areas.

(2) Auquilco Formation

Auquilco Formation consists mainly of gypsum beds accompanied with members of green-colored sandstone, white-colored mudstone and limestone.

Gypsum beds are of white-colored and lack bedding, and vary markedly in thickness. Sandstone is of green-colored, medium-grained and well stratified. Limestone shows lithofacies of dark or brown-colored banded structure and those of resemblance to travertines.

The Formation crops out at La Bramadora area, and ranges in Thickness from 100 to 500 meters. Although it strikes N70°E and dips 30° ~ 40°NW at north, it is assumed to change strike of N-S at south.

(3) Tordillo Formation

Tordillo Formation is mainly composed of members of red-colored sandstone and shale, calcareous siltstone, tuff and limestone.

Red-colored sandstone and shale are of lower members of the Formation and are relatively well stratified. Calcareous siltstone shows greyish white-colored and compact lithofacies, and is interbedded with tuff. Tuff is of yellow-colored, fine-grained dacitic tuff. Limestone shows greyish white-color and rather laminated structure.

The Formation distributes at areas of east of Rincon de Las Papas and south of La Bramadora, and its thickness ranges from 100 to 450 meters. It strikes N40° ~ 50°E and dips 30° ~ 35°NW at northeast, and strikes N30°E ~ E-W and dips 30°NW ~ 20°S at east.

3.2.3 Tertiary Formations

Tertiary formations unconformably overlie on Tordillo Formation of Jurassic, and are composed of andesitic tuff breccia and andesite lava of Miocene to Pliocene in age. Tuff breccia is constituted by andesitic breccia and tuffacious matrix, and flow structure can be observed in lava flows. Both of them are suffered by weak alteration, and show yellow or yellowish grey-color.

The formations crops out at south of Mt. Domo, and their estimated thickness range from 100 to 500 meters.

(2) Granodiorite-porphyry

Tertiary granodiorite-porphyry forms intrusive body cropped out locally at upper stream of Covunco River. Although at its surrounding area dacite lava of younger volcanic rocks distributes, no direct relation between two rocks can be observed.

Lithofacies of granodiorite-porphyry are holocrystalline and porphyritic ones having phenocrysts of chloritized mafic minerals, plagioclase, potash feldspar and quartz.

As is mentioned in the later chapter, it is assumed to be one of the acidic intrusive rocks forming Domuyo Volcano Complex.

3.2.4 Younger Volcanic Rocks

Younger volcanic rocks are roughly divided into andesitic rocks of lower member and dacitic or rhyolitic rocks of upper member.

Andesitic members of younger volcanic rocks occupies northwestern parts of the investigation area, and consists of scoria tuff, pumice tuff, tuff breccia, welded tuff, lapilli tuff and lava ranging in thickness from 200 to 1,000 meters.

Scoria tuff, pumice tuff and tuff breccia show grey-color, and are classified into two types. Namely, one contains plenty of andesite fragments with some of scoria and pumice, and another presents relatively acidic lithology containing a large quantity of pumice. Both of them have mineral pieces of plagioclase and hornblende. Welded tuff is of grey or dark-colored, compact and highly welded tuff, and platy joints in it are commonly observed. Although welded tuff is easily mistaken for glassy andesite because of its appearance, it can

be distinguished from glassy andesite by existences of exotic rock fragments and/or relatively low welded scoria and pumice. Andesite lava is of brown-colored and occassionaly shows flow structure, and platy or columnar joints are common in it. Lapilli tuff crops out at top of Mt. La Papa, and consists of andesitic or a little more basic breccia.

Four dikes of andesite distribute at and near summit of Mt. La Papa striking N-S, dipping vertically and having their widths of 10 meters or more, and continue more than 1 kilometer. Lithofacies of dikes is porphyritic andesite containing less mafic minerlas.

Lava flows of dacite and rhyolite occupy surrounding areas of Mt. Domo and Mt. Covunco and their west. They are composed of dacitic tuff breccia, dacite lava and rhyolite lava from bottom to top, and range in thickness from 200 to 1,000 meters.

Dacitic tuff breccia consists of dacite breccia and tuffaceous matrix, and shows yellowish green or greenish grey-color. Dacite lava contains lenticular thin layers of volcanic glass and shows pinkish brown-color. Flow structure and platy joint are commonly observed in it. Rhyolite lava crops out near top of Mt. Domo, and shows its lithofacies of greyish white-colored pumiceous parts and dark grey-colored fluidal parts.

3.2.5 Glacial Deposits and Alluvium

Glacial deposits, containing angular or subangular breccias of dacite and glassy rock in sandy or tuffaceous matrix, are confined to comparatively small areas at southwestern corner of the investigation area. Unsolid alluvial deposits of sand and gravel are found along Varvarco, Ailinco, Manchana Covunco and Covunco Rivers in the area.

3.3 Petrographic Characteristics of Constituent Rocks

3.3.1 Determination of Absolute Age

(1) Purpose of age determination

In order to make clear volcanism as heat sources which brings on geothermal phenomena, it is important to study its volcano-stratigraphic sequence and history of volcanic activity. Besides, presumptions on rise and fall of magma reservoir and on its thermal ability can contribute to interprete geothermal system. For these purposes, absolute ages of younger volcanic rocks were determined.

In addition, aiming to establish stratigraphic sequence by determinations of absolute age of basement rock, granodiorites were dated.

(2) Results of dating by fission-track method

Datings of younger volcanic rocks were conducted on three specimens of perlite accompanying with lava flows of dacite or rhyolite which belong to Domo volcanics, and on a specimen of welded tuff belonging to Sierra de Flores Formation. Besides, datings of basement rocks were carried out on two specimens of granodiorite taken from central northern and western parts of the area.

Table 3-4 and Table 3-5 show results of examination and dating by fission-track method, respectively.

Table 3-4 Test of fission track data

	Specimen code	No. of grains	Spontaneous tracks		Induced tracks		Coefficient of variation of measured area	Relative standard deviation	F test	
			Average	Coefficient of variation	Average	Coefficient of variation			F value	F^{n1}_{n2} (0.05)
Younger volcanics	DM-1	24	0.7	1.053	332.3	0.191	0.069	0.024	1.38	2.01
	DM-4	(1) 23	1.5	1.267	203.3	0.344	0.257	0.278	2.08	2.05
		(2) 21	1.0	1.023	199.8	0.362	0.248	0.242	1.03	2.12
	DF-1	23	2.0	0.839	204.3	0.248	0.133	0.189	1.27	2.05
	DS-3	25	0.8	1.157	380.0	0.215	0.113	0.241	1.02	1.98
Basement rocks	DM-3	(1) 22	89.1	0.278	75.4	0.178	0.000	0.086	2.60	2.09
		(2) 16	83.6	0.191	74.5	0.168	0.000	0.081	1.37	2.40
	DS-2	(1) 25	95.2	0.317	32.8	0.240	0.000	0.094	2.67	1.98
		(2) 23	94.3	0.250	32.9	0.244	0.000	0.088	1.57	2.05

1) DM-1. Crystals of zircon examined are 24 grains and are colorless. Results of examination give F-value of 1.38 which is better than F-value of 1.50. Because neither heterogeneous grains are found by characteristics of zircon and relation of p_i-p_s nor possibilities of intermix of exotic zircon are considered by microscopic observations, its absolute age is determined on the basis of these examinations.

2) DM-24: Examinations were done for 23 crystals of colorless zircon among total 24 crystals, after previous elimination of a crystal which clearly shows heterogeneous characteristics of older age. As a result of examinations, inferior F-value of 2.08 is obtained. Because 2 grains among 23 crystals show unusual characteristics, which are plotted far from the group in p_i-p_s diagram and contain many inclusions like spontaneous nuclear fission-track, they are also eliminated. As a result of re-examinations, being favorable F-value of 1.03 obtained, its absolute age is determined on the basis of re-examinations.

3) DF-1: Crystals of pale to dark pink-colored zircon examined are 23 grains, and F-value obtained is 1.27. Although a grain is plotted far from the group in p_i-p_s diagram, no unusual characteristics is found in this crystal. Because F-value becomes worse in case the crystal is eliminated, its absolute age is determined on the basis of examinations for total grains.

4) DS-3: Twenty-five crystals of colorless zircon were examined. Although it is anxious about an intermix of exotic crystal microscopically, no unusual chracteristics are found in those of crystal as well as in relation of p_i-p_s. Being good F-value of 1.02 obtained,

its absolute age is determined based on these examinations.

5) DM-3: Crystals of zircon show pale to dark pink-color. As a result of examinations of tataling 22 grains, inferior F-value of 2.60 is obtained. Because the specimen examined is granodiorite of the basement and of geologically old age, there are many inferior crystals of zircon for examinations because of high density of spontaneous nuclear fission-track. Because F-value of re-examinations is improved to 1.37 after eliminations of 6 inferior grains from totaling 22 crystals, its absolute age is determined on the basis of these re-examinations.

6) DS-2: Crystals examined are 25 grains of pale pink-colored zircon. Inferior F-value of 2.67 is obtained. Because there are inferior grains same as those of DM-3, re-examinations of 23 grains after elimination of 2 grains give a little better F-value of 1.57. Although this F-value is not good enough, its absolute age is determined based on these re-examinations.

Table 3-5 Result of fission track dating

	Specimen code	Rock name	Age (Ma)	Character of zircon grains		
				Grain size	Shape	Color
Younger volcanics	DM-1	Perlite	0.11 ± 0.02	200μ < 200 ~ 500μ	Tabular	Colorless
	DM-4	Perlite	0.29 ± 0.07	200μ <		Colorless
	DF-1	Perlite	0.55 ± 0.10	200μ <		Reddish Pale reddish
	DS-3	Welded tuff	0.11 ± 0.03	200μ <		Colorless
Basement rocks	DM-3	Granodiorite	62.66 ± 5.07	200μ < 200 ~ 500μ	Tabular	Pale reddish Reddish
	DS-2	Granodiorite	164.2 ± 14.5	200μ < 200 ~ 500μ		Pale reddish

As a result of datings by fission-track method, absolute ages of younger volcanic rocks indicate to be middle to late Pleistocene in age. Although there is no contradiction generally between ages of dating and those of volcanism assumed by geological survey, some of ages of dating give reverse relations on detailed volcano-stratigraphic sequence.

On the other hand, absolute ages of Varvarco intrusive rocks of the basement are obtained as 62.66 ± 5.07 Ma indicating late Cretaceous to early Paleocene time and 164.2 ± 14.6 Ma indicating middle Jurassic time. These ages are younger than those of Mesozoic formations, which unconformably overlie on the basement and can be correlated to Dogger and Malm

Series of middle to late Jurassic time. Especially, there is a contradiction in facts that Chacay Melehue Formation of the lower-most Mesozoic formation yield ammonite fossils indicating the Bajocian stage of beginning of middle Jurassic time. As is mentioned before, examined crystals of zircon taken from granodiorite include many inferior inclusions showing spontaenous nuclear fission-tracks, and F-values give worse than 2.60. Sufficient F-values are not yet obtained by re-examinations even after eliminations of inferior grains. In connection with alternations converted biotite to chlorite and epidote, it is assumed that spontaneous nuclear fission tracks indicating much older geological ages cannot be enough examined. Therefore, the accuracy of absolute ages of granodiorite obtained by fission-track method is considered to be low.

(3) Results of dating by K-Ar method

Because there are doubts about absolute ages of granodiorite by fission-track method, dating by K-Ar method are employed which method is commonly applied for dating of plutonic rocks such as those of geologically old age, and is considered to have much higher accuracy. Specimens supplied for examinations are DM-2 and DS-1 which are taken from the same points of DM-3 and DS-2, respectively. Examinations were conducted by crystals of hornblende separated from specimens of granodiorite.

Table 3-6 Result of K-Ar age dating

Sample No.	Isotopic age (Ma)	^{40}Ar rad sec/gm X 10^{-5}	% ^{40}Ar rad	% K
DM-2	227 ± 16	0.392	48.3	0.42
		0.397	31.0	0.42
DS-1	259 ± 13	0.837	71.9	0.77
		0.840	74.9	0.78

As a result of datings by K-Ar method, absolute ages of 227 ± 16 Ma of DM-2 and 259 ± 13 Ma of DS-1 indicate boundary between middle and late Triassic time and end of Permian time. This supports the fact of geological age of plutonism that granodiorite intrudes into Choiyoi Group of Permo-Triassic age and unconformably lie under Chacay Melehue Formation of the beginning of middle Jurassic age.

3.3.2 Microscopic Characteristics of Constituent Rocks

(1) Constitutent rocks of the basement

1) Hornfels

Hornfels is originated from sandstone and tuff belonging to Choiyoi Group of Permo-Triassic age. Microscopically, the former consists of abundant quartz-granules with

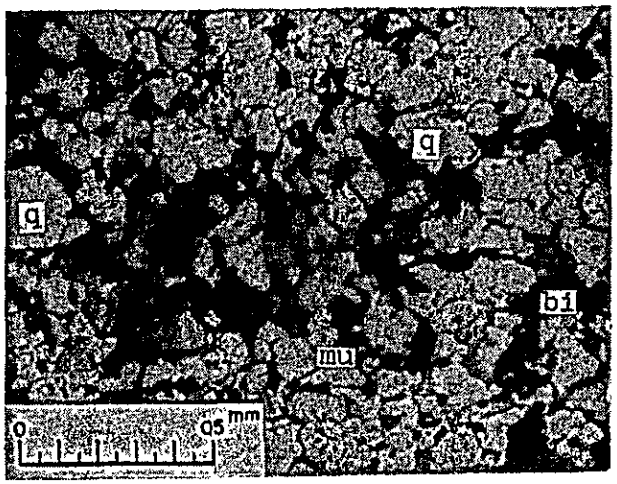

(1) TM-66: Hornfels (sandstone)
(open nicol)

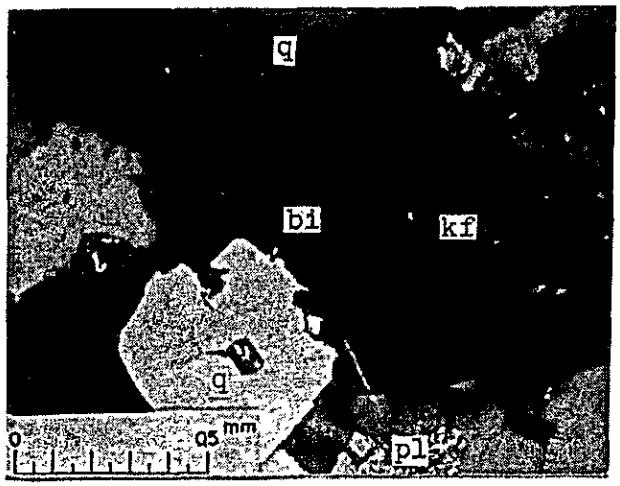

(2) F-26: Granodiorite
(closed nicol)

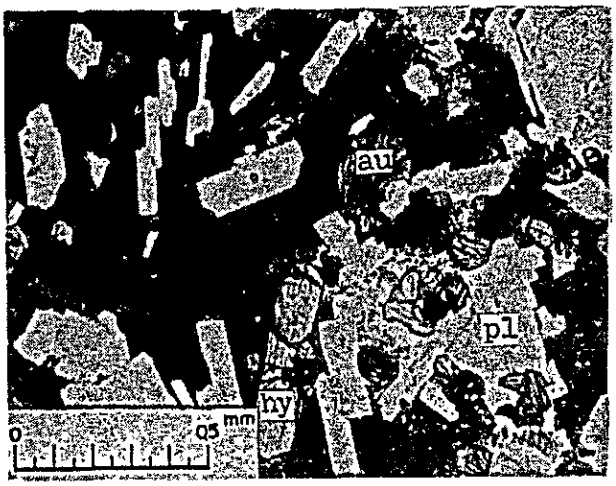

(3) TM-89: Two-pyroxene andesite
(open nicol)

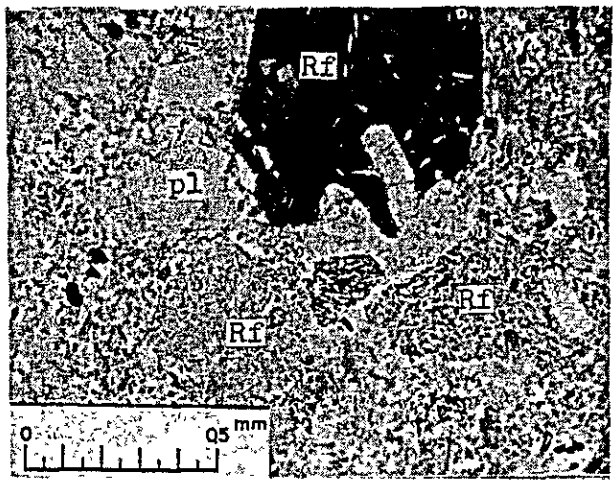

(4) TM-44: Andesitic tuff
(open nicol)

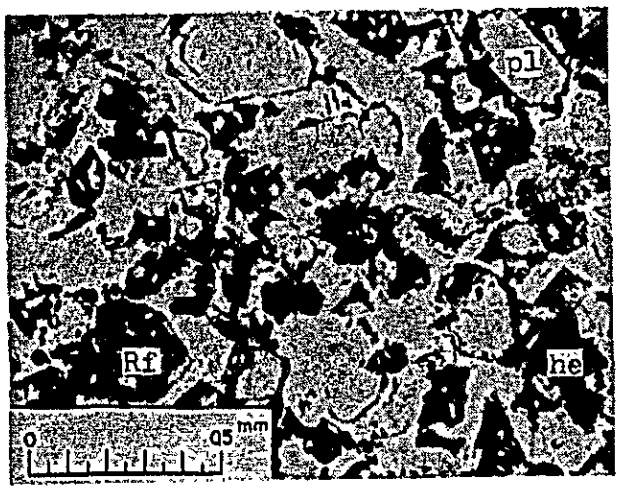

(5) F-33: Tuffaceous sandstone
(open nicol)

EXPLANATION

q : quartz
cr: cristobalite
kf: potash feldspar
pl: plagioclase
mu: muscovite
bi: biotite
ho: hornblende
hy: hyperthene
au: augite
he: hematite
gl: glass

Fe: iron minerals
Rf: rock fragment

Fig. A-2(1)

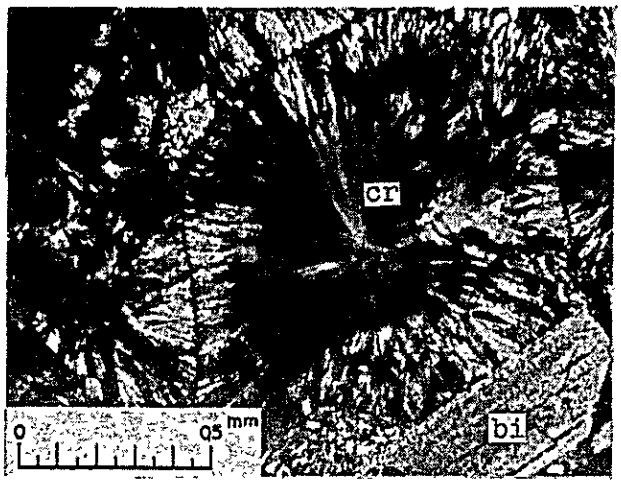

(6) TM-26: Dacite
(closed nicol)

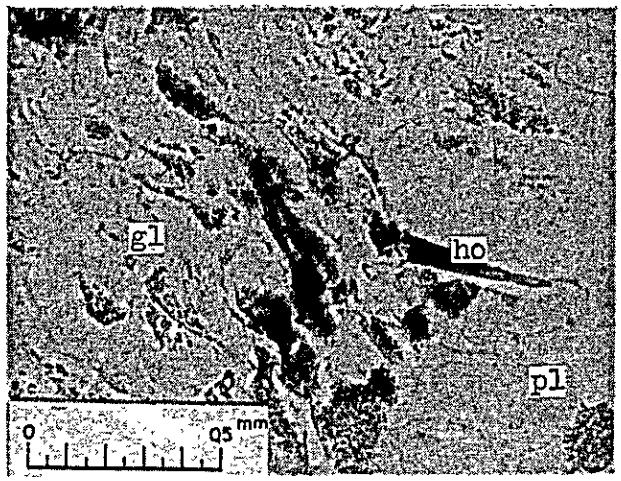

(7) TM-53: Rhyolite
(open nicol)

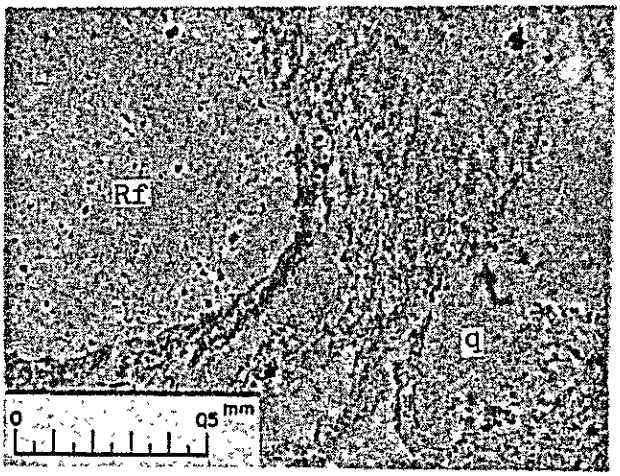

(8) TM-39: Dacitic tuff breccia
(open nicol)

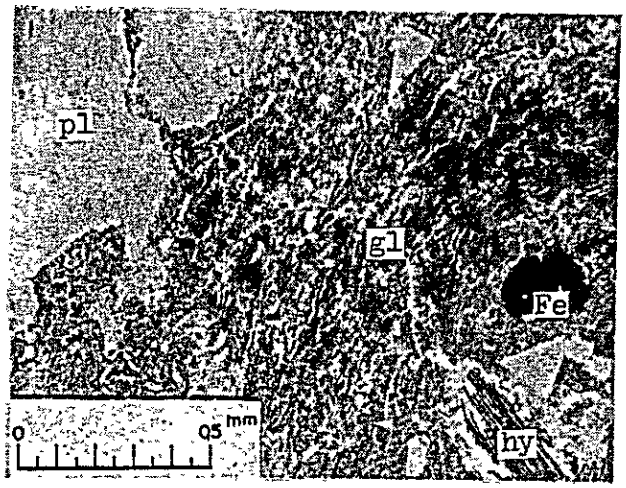

(9) F-3: Dacitic welded tuff
(open nicol)

(10) TM-48: Granodiorite porphyry
(closed nicol)

EXPLANATION

q : quartz
cr: cristobalite
kf: potash feldspar
pl: plagioclase
mu: muscovite
bi: biotite
ho: hornblende
hy: hyperthene
au: augite
he: hematite
gl: glass

Fe: iron minerals
Rf: rock fragment

Fig. A−2(2)

muscovite, hematite and minor amounts of plagioclase, and the later consist of quartz, muscovite and chlorite containing minor amounts of plagioclase and tourmaline. Both of them shown granoblastic texture formed by mosaic of main constituent minerals.

2) Granodiorite

Varvarco Plutonic Rocks, one of basement rocks in the investigation area are represented by hornblende-biotite granodiorite. Microscopically, it is composed mainly of quartz, plagioclase, perthitic K-feldspar and biotite, with subordinate amounts of hornblende. Accessary minerals are minor amounts of iron mineral and a very small quantity of apatite, zircon and sphene. Mafic minerals have mostly been altered into chlorite and epidote, and plagioclases have also been altered into sericite and calcite.

Granodiorites show holocrystalline, equi-granular texture. Most of them are plotted in an area of granodiorite by modal measurements, although some granodiorites are close to mode of tonalite.

3) Aplite

The constituents are quartz, perthitic K-feldspar and plagioclase slightly altered into kaoline and sericite, with accessary biotite mostly altered into chlorite. It shows fine-grained equi-granular texture and partially presents micrographic texture. Aplite is dike rock accompanied with granodiorite intrusions.

(2) Constituent rocks of Mesozoic formations

1) Volcanic rocks and pyroclastic rocks

Among constituents rocks of Mesozoic formations, relatively basic or intermediate volcanic and pyroclastic rocks are dominant in lower formations, and they changes to dacitic lithofacies in portion to upper formations.

Andesite is represented by two-pyoxene andesite which have phenocrysts of plagioclase, augite and hyperthen in a groundmass consisting of plagioclase, secondary quartz, altered mafic minerals and iron minerals. Alterations range intermediate to strong, and are sericitization of plagioclase and chloritization of mafic mineral with partial silicification. Dacite has phenocrysts of quartz and plagioclase in a groundmass of quartz-granules, and is occasionally suffered by strong silicification and sericitization.

Andesitic tuff breccia and lapilli tuff of lower portions consists of large amounts of andesite-fragments. Dacitic ones of upper parts contain dacite-fragments and andesite-fragments, together with mineral-pieces of plagioclase, quartz and minor amounts of altered mafic minerals in a matrix of quartz-aggregates with a little iron mineral. Both of pyroclastic rocks change from fresh to strongly silicified or chloritized.

2) Sandstone

Coarse-grained sandstone is of arkose sandstone consisting of abundant quartz-granules. Fine-grained sandstone consists of quartz and muscovite, and contains a large

quantity of hematite. Tuffaceous sandstone is of medium to coarse-grained, rather andesitic one, and fragments of basalt, andesite and dacite with accessary mudstone and sandstone are common.

3) Limestone

Limestone is of crystalline, and consists of mosaic aggregates of calcite in a scale of less than 1.0 mm.

(3) Constituent rocks of Tertiary formations

1) Andesitic tuff

Andesitic tuff breccia contains relatively abundant fragments of andesite, dacite and purmice with a little amount of sandstone and mudstone, together with mineral-pieces of plagioclase, quartz, biotite, hornblende, augite and iron mineral. A matrix of tuff breccia is rich in glass, and suffers carbonatization. Sandy tuff also contains fragments of andesite, dacite, basalt and pumice, together with the same mineral-pieces as those in tuff breccia. A matrix consists of very fine-grained quartz-aggregates and glassy parts altered into cristobalite.

In general, pyroclastic rocks of Tertiary formations are characterized by large amounts of rock-fragments and mineral-pieces in them.

2) Andesite

Andesite is of rather dacitic andesite. Phenocrysts of plagioclase with accessary augite, hyperthene and/or biotite in a groundmass of very fine quartz-aggregates. It shows commonly hyalopilitic and pilotaxitic textures, and occassionally rather trachytic texture. In general, although andesites are fresh, some of them are suffered by weak silicification, Chloritization and carbonatization.

3) Granodiorite-porphyry

Granodiorite-porphyry crops out locally at small areas southeast of the area. Although dacite lava of younger volcanic rocks distributes at its surrounding area, no direct relation between both rocks can be observed.

Microscopically, it consists of phenocrysts of abundant large-scale plagioclase with accessary mafic minerals in a groundmass of plagioclase, K-feldspar, hornblende, biotite and quartz. It is holocrystalline rock showing micrographic texture, and is suffered locally by carbonatization and chloritization. Lithologically, there is a possibility that the granodiorite-porphyry belongs to one of the intrusive facies of Domuyo Volcano Complex.

(4) Volcanic rocks of late Tertiary to Quaternary age

1) Andesite

Andesite are represented by augite andesite, and include two-pyroxene andesite, hornblende-hyperthene andesite, hornblende andesite etc. Microscopically, phenocrysts are

aboundant plagioclase and subordinate amounts of augite, with accessary hyperthene and hornblende, and rare olivine. A groundmass consists of plagioclase laths with a little amount of augite, hyperthene and iron mineral in a glassy matrix, and shows hyalopilitic, pilotaxitic and intersertal textures. Alterations are generally weak, and kaolinitization, sericitization and/or chloritization are locally observed.

2) Pyroclastic rock ·

Andesitic tuff breccia is of lithic tuff. It contains aboundant andesite-fragments with mineral-pieces of plagioclase and accessary augite and olivine in a matrix of glass with the same mineral-aggregates. No alteration is found.

Scoria tuff is of andesitic tuff contained iron mineral-rich scorias, and changes to a little dacitic lithofacies. Scorias of andesite, dacite and pumice, and mineral-pieces of plagioclase, pyroxene and iron mineral set in a glassy matrix.

All of welded tuff are dacitic, and are divided into two lithofacies of rich in pumice and remarkable in fluidal structure by welding. Fragments of a little amount of dacite, andesite and pumice together with mineral-pieces of plagioclase, augite and quartz are found in a grassy matrix. No alteration is observed.

Pumice tuff contains relatively abundant fragments of pumice and is rich in mineral-pieces of plagioclase and quartz. A matrix is generally glassy.

(5) Younger volcanic rocks of Quaternary age

1) Dacite and dacitic tuff breccia

Microscopically, almost all of dacite are characterized by spherulitic texture of silica mineral. Phenocrysts of abundant plagioclase, subordinate quartz and K-feldspar with accessary biotite, hornblende, hyperthene and rare augite are set in a groundmass of glass with very fine-grained aggregates of silica minerals such as quartz, cristobalite and trydemite.

Dacitic tuff breccia consists of fragments of dacite, pumice with accessary andesite, mineral-pieces of quartz and plagioclase in a matrix of glass and very fine-grained aggregates of cristobalite with a minor amount of quartz and plagioclase.

2) Rhyolite

Rhyolite generally shows flow structure, and partially perlitic structure is observed. Phenocrysts are of plagioclase with accessary hornblende and augite, and a matrix is mostly glassy contained a very little quantity of mineral-aggregate.

3.3.3 Petrographic Characteristics of Holocrystalline Rocks

(1) Classification by mode of Q-Kf-Pl

Holocrystalline rocks in the investigation area are divided into two; namely, granodiorite of Varvarco Plutonic Rocks of the basement and granodiorite-porphyry considered one of the intrusive facies of Domuyo Volcano Complex. As is mentioned before, absolute ages of the former were determined by K-Ar method to be intrusions during the period from

end of Permian age to later half of middle Triassic age. On the other hand, the activity of Domuyo Volcano Complex has been placed in the period from middle Miocene to early Pliocene in age.

Lithofacies and alterations of both holocrystalline rocks under microscope were already described in the former chapter. Fig. 3-6 shows modal diagram of Q-Kf-Pl, based on results of modal measurement on quartz-potash feldspar-plagioclase of these rocks.

As shown in the Fig. 3-6, all of 8 specimens of granodiorite belonging to Varvarco Plutonic Rocks are plotted in a area of granodiorite. Although, they belong to the category of granodiorite, few of them show lithofacies close to tonalite. On the other hand, two specimens taken from intrusive bodies located at the upper stream area of Covunco River, among totaling four specimens of granodiorite-porphyry considered to be one of the intrusive facies of Domuyo Volcano Complex, are plotted in a area of granodiorite being close to that of quartz monzo-syenite. The remainders, which take from rolling stones at middle to lower stream area of Covunco River, are plotted in areas of quartz monzo-syenite and quartz diorite being close to the area of granodiorite.

Thus, as compared with rather homogeneous lithofacies shown by granodiorite of Varvarco Plutonic Rocks which form geologically older batholitic intrusive bodies, lithofacies of granodiorite-porphyry considered to belong to Domuyo Volcano Complex are characterized by their diversities which may be caused by geological environments to form younger hypabyssal intrusive bodies.

(2) Trend of joint system in granodiorite

Joint system developed in granodiorite of the basement is tectonically one of the important factors to reveal trend of fracture system at depths. As shown in Fig. 3-7, trends of joints totaling 78 measurements are predominant in NNE-SSW system striking N20° ~ 30°E, and NE-SW and WNW-ESE system striking N50° ~ 80°W. They are followed by NE-SW, N-S and E-W systems. Relations between trends of joint system and geologic structure assumed by geological survey and gravity prospecting will be mentioned in the later chapter.

3.3.4 Petrographic Characteristics of Younger Volcanic Rocks

Brousse, R. and Pesce, A.H. (1982) studied on chemical characteristics of younger volcanic rocks of Quaternary age distributed in the area of Domuyo Volcano. They reached the following conclusions that younger volcanic rocks can be devided into calc-alkaline series and shoshonitic series on the basis of their alkali-silica contents, and both series are considered to be originated from different volcanic activities by two independent magmas. Namely, the earlier volcanism taken place during late Pliocene to early Pleistocene time is characterized by that of calc-alkaline series, and has yielded andesitic volcanic rocks belonging to Sierra de Flores Formation and others. On the other hand, the later volcanism occurred during middle Pleistocene time is represented by that of shoshonitic series close to alkaline series, and has formed dacitic and/or rhyolitic volcanic rocks belonging to Domo Volcanic

Table 3-7 Chemical compositions of Quaternary volcanic rocks

Sample No.	SiO_2 %	TiO_2 %	Al_2O_3 %	Fe_2O_3 %	FeO %	MnO %	MgO %	CaO %	Na_2O %	K_2O %	$+H_2O$ %	$-H_2O$ %	P_2O_5 %	CO_2 %	LOI %
F 3	66.04	0.84	15.86	2.44	1.87	0.07	1.02	2.78	4.06	4.32	0.33	0.13	0.13	0.08	0.75
F 8	52.28	1.03	18.95	5.23	3.13	0.14	4.01	8.20	2.78	0.76	1.57	0.84	0.16	0.15	2.91
F 23	73.21	0.24	12.54	1.11	0.61	0.11	0.25	0.43	4.71	4.27	1.87	0.31	0.02	0.22	2.78
F 46	65.61	0.87	15.97	3.28	1.22	0.08	0.82	2.63	3.77	4.31	0.50	0.28	0.16	<0.04	1.08
TM 6	65.56	0.90	15.99	3.14	1.44	0.07	0.96	3.04	4.11	4.08	0.16	0.16	0.19	0.26	0.71
TM 13	75.99	0.18	12.75	0.99	0.36	0.08	0.19	0.58	3.85	4.62	0.12	0.08	0.02	<0.04	0.58
TM 20	62.29	0.91	16.14	2.97	2.30	0.14	1.33	3.70	3.89	3.15	1.71	0.32	0.19	0.18	2.79
TM 31	60.22	0.78	17.54	4.14	2.44	0.13	2.21	5.97	3.39	1.72	0.53	0.32	0.15	0.18	1.43
TM 44	63.00	0.82	15.59	3.80	1.87	0.13	0.91	3.20	3.51	3.49	2.22	0.73	0.17	0.11	3.70
TM 45	68.76	0.76	15.31	2.64	0.93	0.09	0.36	2.61	4.55	3.27	0.10	0.17	0.16	0.22	0.71
TM 48	71.69	0.35	14.10	1.35	0.72	0.12	0.35	1.27	3.96	4.52	0.78	0.13	0.08	0.22	1.52
TM 50	75.65	0.23	12.73	1.49	0.29	0.12	0.14	0.27	4.73	4.42	0.04	0.05	0.02	0.07	0.42
TM 52	68.16	0.60	15.00	4.80	0.14	0.07	0.14	1.32	4.06	4.46	0.53	0.15	0.06	0.11	1.14
TM 53	73.73	0.22	12.62	1.23	0.36	0.12	0.14	0.29	4.80	4.31	1.83	0.22	0.02	0.29	2.72
TM 69	60.50	0.66	17.08	4.26	2.01	0.15	2.50	5.67	3.42	1.61	0.78	0.44	0.16	0.07	1.63

Table 3-8 C.I.P.W norm of Quaternary volcanic rocks

	Sample No.	Q	C	F			P		ol	H		ap.	total
				or	ab	an	di	hy		il	hm		
1	F-3	18.86	0	25.53	34.33	12.30	0.51	2.46	0	1.60	0	0.31	99.44
2	F-8	8.73	0	4.49	23.51	36.99	2.13	13.26	0	1.96	0.01	0.38	99.02
3	F-23	28.58	0	25.24	39.83	0.47	1.19	0.08	0	0.46	0	0.05	97.51
4	F-46	20.36	0.70	25.47	31.88	12.01	0	3.63	0	1.65	2.13	0.38	99.88
5	TM-6	18.21	0	24.11	34.76	13.14	0.58	3.40	0	1.71	1.58	0.45	100.20
6	TM-13	34.23	0.41	27.30	32.56	2.75	0	1.13	0	0.34	0.37	0.05	100.04
7	TM-20	18.01	0.06	18.62	32.90	17.12	0	4.88	0	1.73	0	0.45	98.07
8	TM-31	18.50	0	10.17	28.67	27.57	0.83	5.13	0	1.48	0	0.36	98.71
9	TM-44	20.45	0.63	20.63	29.68	14.77	0	5.30	0	1.56	0.99	0.40	98.48
10	TM-45	23.88	0	19.33	38.48	11.70	0.17	1.43	0	1.44	1.89	0.38	99.79
11	TM-48	27.92	0.58	26.71	33.49	5.78	0	2.11	0	0.66	0.18	0.19	99.32
12	TM-50	30.50	0	26.78	40.00	0.46	0.62	0.41	0	0.44	1.03	0.05	100.29
13	TM-52	24.62	1.24	26.36	34.33	6.16	0.00	0.46	0	0.30	4.80	0.14	98.41
14	TM-53	28.57	0	25.47	40.59	0.17	0.96	0.39	0	0.42	0.60	0.05	98.13
15	TM-69	17.88	0	9.52	28.92	26.50	0.36	8.93	0	1.25	0.77	0.43	99.61

Rocks.

As a result of studies done through the second phase survey on volcano-stratigraphic sequence in the investigation area, it was made clear that there are two volcanic activities mentioned by Brousse et al; namely, the earlier volcanism of mainly andesitic volcanic rocks and the later volcanism of dacitic and rhyolitic volcanic rocks. Accordingly, aiming to reveal characteristics of vaolcanism of two stages, a chemical analysis of 15 specimens of younger volcanic rocks was carried out as shown in Table 3-7.

Based on these analytical results, CIPW classification of norm (Table 3-8), relation of alkali-silica contents (Fig. 3-8) and alkali-FeO-MgO compositions (Fig. 3-9) were studied. As shown in Fig. 3-8, all of them range from intermediate rocks of 52 ~ 66% of silica contents. Relations between alkali-silica contents show a positive correlation in an area of calc-alkaline series between boundaries of calc-alkaline and shoshonitic series suggested by Brousse et al. Besides, alkali-FeO-MgO compositions clearly support that chemical compositions of volcanic rocks examined are almost identical with those of representative volcanic rocks of calc-alkaline series.

Thus, it can be said that younger volcanic rocks of Quaternary age in the investigation area belong to calc-alkaline series, and are a sequence of volcanic rocks ranging from intermediate to acidic composition. The age of 0.72 ± 0.10 Ma as the oldest one was previously reported, and their ages of 0.55 ± 0.10 Ma, 0.29 ± 0.07 Ma, 0.11 ± 0.03 Ma and 0.11 ± 0.02 Ma were determined through this study. Accordingly, it is concluded that Quaternary volcanism in the area was various from early to late Pleistocene age, and resulted from a sequence of magmatism of calc-alkaline series ranging from intermediate to acidic composition. And, it is considered that there are no long extinct periods of volcanism, even though some of rise and fall of magmatism may be assumed.

3.4 Physical Properties of Constituent Rocks

A number of rock specimens supplied to laboratory examinations, taken through geological and alteration zone surveys in the field, are shown in Table 3-9, and their locations are shown in Fig. 3-11.

Table 3-9 Numbers of rock specimens

Thin section	X-ray analysis	Physical property					Age dating		Whole rock analysis
		Density	Porosity	Magnetic susceptibility	Resistivity	Thermal conductivity	K-Ar method	Fission track method	
110	142	110	88	62	61	61	2	6	15

In this paragraph, analytical results on physical properties of constituent rocks are presented. Table 3-10 and Fig. 3-11 show all inclusive results of measurement of physical properties and diagram of physical properties of rocks, respecitvely.

3.4.1 Density

Three kinds of density; namely, natural condition, water saturated and oven dry are compared with units of stratigraphical sequence (D, B, J, T, V-1 and V-2 in Table 3-10). Average values of density regularly change from high to low in portion as stratigraphical sequence from the basement (unit B) of bottom to Domo volcanic rocks (unit V-2) of top. Besides, lithologically, the highest density is recorded in metamorphic rocks and granodiorites of the basement, and followed by most of rocks of overlying Mesozoic formations. Among volcanic rocks, densities become smaller from andesite of intermediate composition in order of dacite and rhyolite of acidic composition. Pyrocrastic rocks form a group of low density. Among them, scroria tuff and pumice tuff of younger volcanic rocks have the lowest density.

3.4.2 Porosity

There is a good negative correlation between effective porosity and density. Quaternary pyroclastic rocks of low density show first-class high effective porosity of more than25%. However, welded tuff, a member of Quaternary pyroclastic rocks, have high density as more than 2.5 g/cm^3 and low effective porosity as 3%, because of its high-grade welding. Most of Mesozoic rocks and basement rocks have low values of less than 5%.

3.4.3 Susceptibility

The lowest susceptibility is of basement rocks. Rocks of Mesozoic formations except basalt and/or andesite as well as acidic volcanic rocks of unit V-2 have low values of susceptibility as less than 500 X 10^{-6} emu/cc. This supports relations between lithology and usual values of susceptibility. The highest susceptibility is measured in andesits and their pyroclastic rocks of Tertiary formation (unit T) and earlier Quaternary volcanic rocks (unit V-1), and values are high as more than 1,000 X 10^{-6} emu/cc. The facts are caused by high contents of magnetite in andesite. And, as is mentioned in paragraph of microscopic characteristics of constituent rocks, andesitic pyroclastic rocks contains abundant andesite-fragments of high susceptibility.

3.4.4 Resistivity

FE values show mostly 1.5 ~ 2.0%, and maximum and minimum FE values are 3.8% and 0.7%, respectively. These values are of common rocks. The highest value of resistivity is of basement rocks, followed in order of values by volcanic rocks, sedimentary rocks and pyroclastic rocks. These values of resistivity are rather high compared with those of common rocks. As this cause, it is considered that rock specimens supplied to laboratory ecaminations are of representative rocks selected from each lithofacies, and are of fresh rocks without any alterations related to geothermal phenomena. On the contrary, this fact may suggest that vertical electric prospecting is effective in the area in order to study alteration zones of low resistivity formed by geothermal phenomena.

Table 3-10 All inclusive results of measurement of physical properties (the mean value of rock facies & geological unit)

Rock facies	Geological unit		Density (g/cm^3)						Porosity		Susceptibility		Resistivity				Termal conductivity	
			Natural condition		Water saturated		Oven dry		(%)		(emu/cm^3) x 10^{-6}		FE (%)		ρ (Ω-m)		(cal/cm.sec.°C) x 10^{-3}	
			R.f	G.u	R.f	G.u	R.f	G.u	R.f	G.u	R.f	G.u	R.f	G.u	R.f	G.u	R.f	G.u
Rhyolite	V	V-2	1.78	2.19	1.85	2.26	1.77	2.16	7.79	8.00	184	298	1.6	1.9	2854	1861	1.687	2.708
Dacite			2.25		2.31		2.21		7.42		360		2.2		1097		2.633	
Dacitic tuff breccia (1)			2.09		2.21		2.04		16.58		-		-		-		-	
Dacitic tuff breccia (2)			2.17		2.25		2.19		7.58		250		1.7		2728		3.541	
Pumiceous tuff		V-1	1.40	2.22	1.70	2.32	1.38	2.18	32.18	13.33	1170	1290	-	1.4	-	465	0.582	2.793
Welded tuff			2.54		2.56		2.53		3.10		1185		1.3		537		3.576	
Andesitic tuff breccia			2.00		2.17		1.92		25.07		1119		1.3		62		2.529	
Scoriaceous tuff			1.91		2.06		1.86		21.24		812		1.7		95		1.709	
Andesite			2.48		2.52		2.48		5.86		1635		1.2		712		3.542	
Andesite	T		2.47	2.35	2.50	2.41	2.43	2.22	4.48	11.08	1503	855	1.7	1.6	3219	1929	3.944	4.335
Andesitic tuff breccia			2.13		2.23		2.07		16.04		370		1.5		961		4.725	
Sandstone, Mudstone	J	J-3	2.54	2.03	2.56	2.15	2.53	1.99	3.03	15.54	62	112	1.5	1.6	335	174	5.522	3.609
Tuff			1.68		1.87		1.63		23.88		145		1.6		67		2.333	
Sandstone		J-2	2.41	2.52	2.47	2.56	2.40	2.51	6.84	4.53	27	-	3.2	-	357	-	6.690	-
Limestone			2.62		2.64		2.62		2.22		-		-		-		-	
Sandstone, Mudstone (Basalt)		J-1	2.64	2.54	2.65	2.56	2.63	2.51	1.98	4.36	68	277	1.7	1.7	468	2999	6.100	6.088
Andesite, Basalt			2.52		2.56		2.51		5.46		602		1.6		582		5.463	
Pyroclastic rocks			2.51		2.54		2.45		4.91		138		1.8		6078		6.552	
Granodiorite	B		2.66	2.66	2.67	2.67	2.66	2.66	1.06	0.94	187	116	1.9	2.0	1853	4858	7.539	9.057
Metamorphosed rocks			2.69		2.70		2.69		0.63		41		1.9		11243		12.577	
Aplite			2.61		2.61		2.60		1.19		52		2.5		2795		7.575	
Andesite dyke	D		2.46	2.52	2.49	2.54	2.44	2.52	5.72	3.73	-	429	-	2.1	-	5550	-	7.277
Basalt dyke			2.66		2.67		2.66		1.27		55		1.3		9911		9.457	
Granodiorite porhyry			2.46		2.48		2.45		3.21		803		2.8		1189		5.098	

V: Quaternary-Tertiary

V-2: Pleistocene, Volcanics of Co. Demo

V-1: Pleistocene-Pliocene,
Acidic Pyroclastics
Sierra de Flores Formation
Atreuce Formation

T: Tertiary, Pliocene-Miocene,

J: Jurassic, Dogger-Malm,

J-3: Tordillo Formation

J-2: Auquilco Formation

J-1: Chacay Melehue Formation

B : Basement

D : Dike Rock, etc.

R.f: Rock facies

G.u: Geological unit

3.4.5 Thermal Conductivity

Because older rocks such as basement rocks and/or Mesozoic formations have been highly consolidated in comparison with younger rocks such as Quaternary volcanic rocks, values of thermal conductivity range generally from high at lower sequence to low at upper sequence. Accordingly, thermal conductivity has a positive correlation with density and a negative correlation with effective porosity. Values of thermal conductivity of rocks from upper horizons than unit J-2 of Mesozoic formation are of usual as $2 \sim 5 \times 10^{-3}$ cal/cm·sec.°C. However, those of rocks from unit J-1 of Mesozoic formation, unit B of basement and unit D of dike show fairly higher than common values.

3.5 Summary of Geology

(1) Geology of the investigation area is divided into four units. Namely, the basement consists of metamorphic rocks such as crystalline schist and hornfels belonging to Choiyoi Group of Pesmo-Triassic age and of granodiorite of Varvarco Plutonic Rocks. Mesozoic formations of Jurassic age, Chacay Melehue Formation, Auquilco Formation and Tordillo Formation in ascending order, unconformably overlie on the basement. Tertiary formations of Miocene to Pliocene age follows unconformably, and granodiorite-porphyry concidered to be a member of intrusive facies of Domuyo Volcanic Complex is locally distributed at southeastern parts of the area. Younger volcanic rocks, occured during periods from end of Tertiary to Quaternary time, are composed of lava flows of andesite, dacite and rhyolite erupted from earlier to later stage, and are accompanied with their pyroclasitic rocks.

(2) Absolute ages of younger volcanic rocks determined by fisson-track method range from 0.55 ± 0.10 Ma to 0.11 + 0.02 Ma. These ages together with 0.72 ± 0.10 Ma of previous data indicate that Quaternary Volcanism took place during periods from early to late Pleistocene time. Absolute ages of granodiorite of the basement determined by fission-track method are doubtful because of their younger ages than geological age of unconformably overlying Mesozoic formations indicated by ammonite fossils. However, as a result of datings by K-Ar method, absolute ages of granodiorite are determined as 227 ± 16 Ma and 259 ± 13 Ma. These ages are of late Permian and end of middle Triassic time, and support stratigraphic sequences in the investigation area.

(3) Holocrystalline rocks in the area are composed of granodiorite of Varvarco Plutonic Rocks of the basement, and of granodiorite-porphyry to be considered a member of intrusive facies of Domuyo Volcano Complex. As a result of measurements of Q-Kf-Pl mode, as compared with all of the former show rather homogeneous lithofacies of granodiorite, the later has some deversities of their lithofacies ranging from granodiorite to quartz monzosyenite and quartz diorite.

(4) Based on a chemical analysis of younger volcanic rocks, it is revealed that Quaternary volcanism taken place during periods from early to late Pleistcene age is characterized by a

sequence of magmatism of calc-alkaline series ranging from intermediate to acidic composition.

(5) Regarding physical properties of constituent rocks in the investigation area, the following results are obtained.

Density changes regularly from high to low in portion of the basement at bottom of sequence to younger volcanic rocks at top of sequence, and the lowest density is of pyroclastic rocks such as scoria tuff and pumice tuff. Effective porosity has good negative correlation with density. And its values show low percentage in basement rocks and Mesozoic formations, and high percentage in Quaternary pyroclastic rocks. Values of susceptibility are high in andesites and their pyroclastic rocks among Tertiary and Quaternary volcanic rocks, and generally correspond to lithofacies. As compared with FE values shown those of usual rocks, values of resistivity are relatively high which the highest value is of basement rocks followed in order of values by volcanic rocks, sedimentary rocks and tuffs. Values of thermal conductivity are higher in rocks of lower sequence and become lower in portion of in rocks of upper sequence, and fairly higher values than common cases are obtained from lower half of Mesozoic formations and basement rocks.

4. Geologic Structure in the Investigation Area

4. Geologic Structure in the Investigation Area

4.1 Geologic Structure based on Geological Distributions and Physical Properties of Constituents Rocks

4.1.1 Geologic Structure Based on Geological Distributions

Geological distributions in the investigation area show remarkable differences between eastern half and western half being roughly bordered by a line of N-S direction from El Humazo to Los Tachos.

Namely, in western half of the area, metamorphic rocks belonging to Choiyoi Group of Permo-Triassia age and granodiorites belonging to Varvarco Plutonic Rocks are located at rather shallow parts, and overlying younger volcanic rocks are widely distributed. Basement rocks of metamorphic rock and granodiorite crop out along Varvarco River and others like windows beneath younger volcanic rocks. It is assumed that nearly flat erosion surface of the basement formed paleotopography which even has some of unevenness.

On the other hand, in eastern half of the area, no basement rocks crop out, and basements of younger volcanic rocks consist of Mesozoic formations.

Mesozoic formations, distributed in the central parts of areas between El Humazo and upstreams of Manchana Covunco, strike N30°E ~ N30°W and dip 15° ~ 30°E. They are structurely harmonious with western wing of southern extension of N-S synclinal axis at west of El Turbio (cf. Fig. 2-2). In opposit, Mesozoic formations, distributed in an area between west of Rincon de Las Papas and southeast of Mt. Domo, occupy eastern wing of the same synclinal axis. Because this area is a western part of large-scale box-shaped dome structure centering around Domuyo Volcano, essential structure strikes N-S and dips towards west. However, under the influence of local doming-up at areas of Mt. Domo, some structural disturbances appear striking NW-SE ~ E-W and dipping towards northwest at northeastern area, and strikingNE-SW ~ NNE-SSW and dipping towards southeast at southeastern area.

Although Tertiary formations unconformably overlie on Mesozoic formations, there are no large structural gaps.

Besides, younger volcanic rocks erupted and flowed on basement rocks, Mesozoic and Tertiary formations. Their structures on and near the surface are generally harmonious with those of underlying older rocks, even though their lava flows were controled by unevenness of paleotopographic surface.

Fault systems developed in the investigation area are dominant in N-S and NW-SE systems accompanied with NE-SW system, which correspond regional fault systems of N-S and E-W systems of large-scale and of NE-SW and NW-SE systems of a little small-scale.

As is mentioned in the latter chapter, it is assumed that major faults of N-S system exist at a little western part of southern extension of Turbio synclinal axis where Bouguer values of gravity changes suddenly along or parallel to the axis. Although this assumed fault of N-S system bent toward SE or SSE directions near Mt. Domo area, it can be considered to be major fault zone combined by faults of N-S and NW-SE systems.

4.1.2 Subsurface Structure based on Physical Properties of Constituent Rocks

Densities of constituent rocks of the area change regularly from high in basement rocks of the oldest age to low in Domo volcanic rocks of the youngest age. Subsurface structure in western half of the area, based on density of constituent rocks in relation with geological distributions, forms two-layered structure composed of high density layer having 2.6 ~ 2.7 g/cm^3 of basement rocks and of low density layer showing approximately 2.3 g/cm^3 of overlying younger volcanic rocks. On the other hand, in eastern half of the area, two layered structure is also formed consisting of low density layer of younger volcanic rocks and of medium density layer having 2.4 ~ 2.6 g/cm^3 of underlying Tertiary and Mesozoic formations. However, high density layer of basement rocks is assumed to be latent at depths.

Thus, although both halves of the investigation area are characterized by each two-layered structure consisting of younger volcanic rocks at upper sequence and older rocks at lower sequence, there are locally differences on balance of densities such as 0.3 ~ 0.4 g/cm^3 in western half and 0.1 ~ 0.3 g/cm^3 in eastern half.

Subsurface structure based on effective porosity can be roughly divided into two layers; namely, lower layer having low percentage of effective porosity of basement rocks and lower members of Mesozoic formations and upper layer showing high percentage of effective porosity of upper members of Mesozoic formations and Cenozoic formations. However, the upper layer shows a little more complicated subsurface structure, because changes between lithofacies are remarkable and can be divided into many sub-layers.

Subsurface structure, based on susceptibility, resistivity and thermal conductivity, is considered to be normal in relation with stratigraphic sequence and lithofacies of constituent rocks.

4.2 Underground Structure Presumed by Gravity Anomaly

4.2.1 Gravity Prospecting

(1) Measurement of gravity

LaCoste & Romberg gravity meter model G204 was employed for measurements of gravity. This gravity meter made in 1969 has its measurement scope of 0 to 7261.53 mgal. Table 4-1 shows miligal values foı LaCoste G204 gravity meter.

Gravity in the investigation area was measured at totaling 316 points, which measuring intervals are standarlized each 800 meters apart. In central parts of the area to be considered promising for geothermal prospectings based on geological and geochemical surveys, more detailed measurements were done by reduced measuring intervals of approximately 400 meters apart.

Besides, aiming to study regional gravity distributions, 31 measuring points along survey routes of totaling 1,050 line kilometers in areas between the investigation area and Chos Malal located 80 Km south of the area.

Table 4-1 Milligal Values for LaCoste G204 Gravity Meter

Counter Reading	Value in Milligals	Factor for Interval	Counter Reading	Value in Milligals	Factor for Interval
	K	k		K	k
2,500	2,588.51	1.03713	3,100	3,211.01	1.03802
2,600	2,692.22	1.03727	3,200	3,314.81	1.03818
2,700	2,795.95	1.03741	3,300	3,418.63	1.03835
2,800	2,899.69	1.03756	3,400	3,522.46	1.03852
2,900	3,033.45	1.03771	3,500	3,626.31	1.03870
3,000	3,107.22	1.03786			

(2) Standard of gravity value

Base station of gravity measurement was set at front of No. 4 beungalow in base camps of this survey, and given No. 1,000 (Fig. 4-2b). Gravity value of the base station No. 1,000 was decided on the basis of gravity value of 979,964.02 mgal at the gravity control point 9310-68 (latitude 38°58'S, longitude 68°03'W and altitude 270m) established in the Neuquén Airport (Fig. 4-2a). This gravity value is based on that of International Gravity Standard Network 71.

Table 4-2 gives process to calculate gravity value at the base station No. 1,000. Because periods of gravity prospecting ranged long time from Jan. 14 to Mar. 1, final gravity value at base station No. 1,000 was calculated as 979,375.44 mgal based on three values measured during the periods.

(3) Leveling

Nos. 1 to 142, Nos. 301 to 376 and Nos. 501 to 598 were given for totaling 316 measuring points (cf. Fig. 4-3). Measuring points of Nos. 1 to 142 are located in western highlands, and 137 points among them were surveyed before the prospecting by Argentine team using radio survey meter (Tellurometer CA1000) and Transit (Wild T-2). The remainder of 5 points were surveyed their altitudes by Japanese team using precise altimeter (Paulin Precision Altimeter MM-1) because of difficulty for leveling by radio survey meter. Measuring points of Nos. 501 to 598 are located in eastern mountains of very steep topography. Because of its topography, levelings were done by Japanese team using autolevel meter (Sokkisha Autolevel B-2) for 18 points along valley and precise altimeter for remainder of 80 points. Measuring points of Nos. 301 to 376 were added at detailed survey area of central parts, and leveled by Japanese team using autolevel meter.

Standard point of altitude 1,874 m located 300 m west of the base camps was tentatively used. However, as a result of surveying between the tentative standard point and bench mark RF85N (149) of altitude 1,042.770 m established at Route No. 40 between Barrancas and Butaco, it was become clear that altitude of the standard point shown in topographic map is approximately 67 m higher than true altitude. Therefore, altitudes of each measuring

points leveled in the fields were corrected through data processing. Fig. 4-3 shows routes of leveling.

(4) Observation of tidal variation

Aiming to obtain basic data for determination of coefficient of tidal correction, observations of diurnal gravity variation were done by LaCoste gravity meter during 17 hours on Feb. 11 at the base camp and 14 hours on Feb. 24 at Covunco River. Fig. 4-4 shows results of these observations. Results of observations are fully identical with theoretical curve. Because coefficient of tidal correction of 1.20 suggests to be appropriate, in this area, this coefficient of 1.20 was employed for calculations of tidal correction.

4.2.2 Density for Bouguer Correction

(1) Density of rock specimen

Three kinds of density were measured on total 108 rock specimens taken in the investigation area. These results are given in Table A-2 of appendix, and average densities of each stratigraphic sequences and lithofacies are presented in Table A-3. Among three kinds of density, water saturated density is considered to be very close to natural conditions.

As shown in Table A-3, the highest density is of metamorphic rocks of the basement, and values 2.70 g/cm^3. It followed by granodiorite of the basement having 2.67 g/cm^3. Rocks of Mesozoic formations have densities of 2.47 ~ 2.65 g/cm^3 except tuff showing low density as 1.87 g/cm^3. Sandstone and mudstone of Chacay Melehue Formation and limestone of Auquilco Formation have rather high densities of 2.65 g/cm^3 and 2.64 g/cm^3, respectively. An average density of Mesozoic formations is 2.56 g/cm^3.

Average densities of Tertiary formations and younger volcanic rocks have a tendency to decrease in proportion as geologically younger ages. Among younger volcanic rocks, relatively high densities are given by Tertiary andesite of 2.50 g/cm^3, Quaternary andesite of 2.52 g/cm^3 and Quaternary welded tuff of 2.56 g/cm^3. On the contrary, low densities are obtained from scoria tuff of 2.06 g/cm^3, pumice tuff of 1.70 g/cm^3 and rhyolite of 1.85 g/cm^3 of Quaternary pyroclastic and volcanic rocks. An average density of all of younger volcanic rocks is 2.32 g/cm^3.

(2) g-H relation

Fig. 4-5 shows relations between gravity and altitude. Density based on g-H relation is 1.76 g/cm^3, which calculated by a gradient of straight line connected plotted dots. This value is of very low in comparison with densities measured of rock specimens. The reasons why both densities is not entirely identical, as is mentioned later in more details, can be considered as follows; There is a negative correlation between topography and Bouguer anomaly which is presented by low Bouguer anomalies at eastern mountains. The negative correlation acts as low density of g-H relation.

Besides, distributions of plotted dots in Fig. 4-5 are not completely straight line, but gently curved. Therefore, it seems to be aggregates of several straight lines having different

Table 4-2 Calculations of gravity value at base station No. 1000 in Base Camp

[LaCoste G-204]

Y M D	NO	TIME	READING	INST.H	x FACT.	ETCOR	INST.COR	+ COR	DRIFTCOR	GRVTY DIF.	GRVTY VAL.
		H M		CM	MGAL	MGAL	MGAL	MGAL	MGAL	MGAL	GAL
83 1 14	9310 -68	10 07	3479.020	27.5	3604.522	.019	.085	3604.626	0.000	0.000	979.96402
1 17	1000	8 21	2912.126	27.0	3016.033	-.070	.083	3016.046	-.033	-588.613	979.375407
2 3	1000	8 00	2912.261	27.0	3016.173	.039	.083	3016.295	-.227	-588.558	979.375462
2 18	1000	7 56	2912.440	27.0	3016.359	.020	.083	3016.462	-.398	-588.562	979.375458
3 1	9310 -68	17 45	3479.529	27.5	3605.051	.018	.085	3605.154	-.528	0.000	979.96402

1111 38 DRIFT RATE: 0114 MGAL/DAY

AVERAGE VALUE = (979.375407 + 979.375462 + 979.375458)/3 = <u>979.375442</u>

gradients shown by break lines in figure. Densities obtained from inclines of break line are 2.02 ~ 2.28 g/cm^3, which are closer to measured densities of rock specimens.

(3) Determination of density for Bouguer correction

A correction density ρ of 2.30 g/cm^3 was selected for analyses of Bouguer anomaly. In order to determine density for Bouguer correction, studies were conducted on measured densities of rock specimens, density by g-H relation and three kinds of maps regarding different Bouguer anomalies.

Correction densities used for three Bouguer anomaly maps are 2.00, 2.30 and 2.50 g/cm^3, respectively. Although Bouguer anomalies considered to be influenced by topography are found in case of ρ = 2.00 g/cm^3, no Bouguer anomalies influenced by topography are shown in case of ρ = 2.30 and 2.50 g/cm^3. Finally, the correction density of ρ = 2.30 g/cm^3 was selected which corresponds to an average density of 2.32 g/cm^3 of younger volcanic rocks.

4.2.3 Analytical Results of Gravity Prospecting

(1) Regional Bouguer anomaly

Fig. 4-6 shows regional Bouguer anomaly in southern area to the investigation area. Although this gravity prospecting was done aiming to study gravity trends in the area regionally, it was impossible to conduct in neighborhood of the area because of lack of roads. Therefore, based on results of gravity prospecting in extensive areas, an attempt to presume gravity trends in the investigation area was done.

Bouguer anomaly map of Fig. 4-6 is of without topographic correction. However, general trends of gravity distribution can be made clear, and their characteristics are pointed out as follows;

i) Bouguer anomaly values are of remarkably minus.
ii) It is a tendency to decrease Bouguer anoamly values towards north.

Remarkable minus values of Bouguer anomaly have been detected in high mountains such as Himalayas and Andes. This phenomena are interpreted by the isostasy that earth crusts consisting of rather light materials in comparison with materials of mantle are generally thick at high mountains. The area of regional gravity prospecting is located in a region within 100 Km east of Andes bordering between Argentine and Chile. Although Andes high as more than 5,000 m at north are not so high enough in this region, it is assumed on the basis of remarkable minus values of Bouguer anomaly that the isostasy is still existing in the region.

In general, distributions of Bouguer anoamly can be divided into high and low gravity areas; namely, two high gravity areas centering around El Cholar ~ La Primavera and southeast of Auquinco, and low gravity area extending from Chos Malal to Lake Tromen between two high gravity areas. These anomalous areas are quite in agreement with geological distributions shown in Geological interpretation map of Landsat image of Fig. 2-1. That is, high

gravity area and low gravity area correspond to distributions of pre-Tertiary formations and of Cenozoic volcanic rocks, respectively.

Although values of Bouguer anoamly decrease locally toward east or west, it is a tendency to decrease their values toward north regionally. It is considered that this trend continues as far as the investigation area.

(2) Bouguer anomaly in the investigation area

Fig. 4-7 shows Bouguer anomaly map of ρ = 2.30 g/cm^3, and for reference Fig. 4-8 and Fig. 4-9 give Bouguer anomaly maps of ρ = 2.00 and 2.50 g/cm^3. On the basis of Fig. 4-7, Long-wave Bouguer anoamly map and Short-wave Bouguer anomaly map are made by filter analyses, and presented in Fig. 4-10 and Fig. 4-11. Gravity anomalies of approximately less than 500 m in diameter are selected in Fig. 4-10, and removed in Fig. 4-11. Fig. 4-12 shows three-dimensional image of Bouguer anomaly made on the basis of Fig. 4-7.

Values of Bouguer anoamly based on ρ = 2.30 g/cm^3 in the investigation area range from −162 mgal to −127 mgal. These minus values are caused by the isostasy, as is mentioned before. Bouguer anomaly in the area clearly shows its tendency of high in western parts and low in eastern parts. Because this trend of E-W direction does not correspond to regional trend of N-S direction, it is considered that the trend of E-W direction is that locally developed in and near the investigation area. Besides, although regional trend of N-S direction is not so clear in the area, there are differences of approximately 5 mgal between southern and northern borders of the area, and this seems to indicate regional trend.

The investigation area can be roughly divided into three districts based on gravity distributions.

1) A-district

A-district occupies approximately three-fifth west of the area, and is high gravity area having values of Bouguer anomaly more than −140 mgal. This district is characterized by relatively high Bouguer anomaly and generally small gravity gradient, and furthermore this district can be subdivided into three blocks.

A-1 block occupies northern area from a line connected between El Humazo and Banos del Agua Caliente. This block is characterized by homogeneous and gentle gravity distributions, except northwesternmost parts, and by small gravity gradient of less than 2 mgal/Km. At northwestern parts, values of Bouguer anomaly decrease toward northwest. In this block, gravity distributions of NW-SW and N-S direction can be read from long-wave and short-wave Bouguer anomalies, respectively.

A-2 block is located at central parts of the investigation area, and forms local low gravity anomaly. According to long-wave Bouguer anomaly map, this low gravity anomaly presents a shape of isosceles triangle having the base connecting between El Humazo and Los Tachos and the top near the base camps. Numerous geothermal manifestations such as El Humazo, Las Olletas, Aguas Calientes, Banos del Agua Caliente and Los Tachos are located at marginal parts of this low gravity anomaly.

A-3 block is situated at southern parts of the A-district. This block consists of three local high gravity anomalies elongating with NE-SW direction and two local low gravity anomalies, and presents an area having some changes of gravity distribution among A-district. From gravity contour lines, components of NE-SW direction together with of N-S direction are read.

2) B-district

B-district forms long and slender belt of N-S direction being placed between A and C-districts, and corresponds to transition zone to change from high Bouguer anomalies to low Bouguer anomalies. As shown by dense gravity contour lines, it is characterized by very large gravity gradient which has approximately 6 mgal/Km in average and maximum more than 10 mgal/Km. Graavity gradient in such transition zones usually becomes maximum along its center line. However, in case of the zone, there are two largest places near eastern and western rims. Directions of gravity contour lines are dominant in N-S at most of northern half, and changes to NW-SE at southern part.

3) C-district

C-district forms low gravity area elongating with N-S direction along eastern margines of the investigation area, and has values of Bouguer anomaly of approximately less than −150 mgal. Because it is a tendency to decrease their values toward east except a portion, it is clear that this low gravity area widely extends farther east of the investigation area. In this district, large numbers of gravity anomaly distribute locally, as shown in short-wave Bouguer anomaly map. Although remarkable regularity cannot be seen in these local anomalies, it trends to arrange with N-S direction at areas near B-district.

(3) Qualitative analysis

Gravimetric interpretation map of Fig. 4-14 shows results of qualitative analysis on Bouguer anomaly of $\rho = 2.30$ g/cm^3.

As a result of the analysis, the area was generally classified to areas of high gravity and low gravity, based on values of Bouguer anomaly. Then, local structures such as gravity lineament, gravimetric anticlinal and synclinal structures were selected on the basis of pattern of gravity distribution. Gravimetric lineaments are linear structures distinguished from gravity distributions. There are lineaments parallel and oblique to contour lines. Gravimetric anticlinal and synclinal structures are represented by local gravity anomalies elongating like roof-shaped high anomaly and valley-shaped low anomaly, respectively.

The results shown in Fig. 4-14 is mentioned in details in next paragraph 4.3 Considerations on Geologic Structure, in relation with geological interpretations on gravity distributions.

(4) Quantitative analysis

Fig. 4-15, Fig. 4-16 and Fig. 4-17 show calculative results on depth of two-layered

structure along A-A', B-B' and C-C' cross-sections.

A hypothesis of two-layered structure is based on younger volcanic rocks as upper layer of lower density, and metamorphic rocks and granodiorite of the basement and Mesozoic formations as lower layer of higher density. Balances of density are set by 0.2, 0.4 and 0.6 g/cm^3 for A-A' cross-section and by 0.2, 0.4, 0.6 and 1.0 g/cm^3 for B-B' and C-C' cross-sections. Among these numbers, 1.0 g/cm^3 indicates difference between pumiceous tuff and granodiorite, and 0.6 g/cm^3 indicates difference between scoria tuff and granodiorite. The remainding 0.2 and 0.4 g/cm^2 are not supposed for special rocks or formations, but they are selected for calculations to study depth of gravity basement.

At top of Fig. 4-15, Fig. 4-16 and Fig. 4-17, profile of Bouguer anomaly of ρ = 2.30 g/cm^3, long-wave Bouguer anomaly and calculated values of gravity anomaly by $\Delta\rho$ = 0.2 g/cm^3 are shown. Calculated values of gravity anomaly by $\Delta\rho$ = 0.2 g/cm^3 are presented for examples of the largest deflection between calculated values and measured values. Calculated values of Bouguer anomaly by other balances of density fit with measured values in comparison with case of $\Delta\rho$ = 0.2 g/cm^3. In middle of each figures, average densities corresponding to each formations and lithofacies are given. And, at bottom of each figures, calculated results by each balances of density are presented.

In addition, points where granodiorite crops out are selected as control points for calculations. Detailed interpretations on quantitative analysis of gravity anomaly are mentioned in next paragraph 4.3 Considerations on Geologic Structure.

4.3 Considerations on Geologic Structure

4.3.1 Relation between Geology and Gravity Anomalous Area

As shown in Fig. 4-14, distributions of Bouguer anomaly in the investigation area are clearly divided into high gravity area at west and low gravity area at east, and medium gravity belt exists between them. High and low gravity areas correspond to A and C-districts classified by gravity distributions, and long and slender transition zone having intermediate gravity corresponds to B-district.

In attempting to correlate geological map and Bouguer anomaly map, it is difficult to find out relevancy between distributions of Quaternary younger volcanic rocks covering widely in the investigation area and general classifications by gravity anomaly of high at west, low at east and intermediate at the middle. As is mentioned latter, only local relevancy is recognized between distribution of pumice tuff and low gravity anomaly in A-district.

Accordingly, as geological factors to form gravity anomalous areas, it is necessary to consider geologic structure of basement rocks and Mesozoic formations except geology of younger volcanic rocks.

In A-district at west corresponding to high gravity area, granodiorites crop out along rivers of Varvarco, Manchana Covunco and Covunco, and metamorphic rocks expose at areas of Manchana Covunco River. Thus, it is assumed by geological survey that these basement rocks are widely distributed beneath younger volcanic rocks of Quaternary age. Because

metamorphic rocks have the highest density of 2.70 g/cm^3 and are followed by granodiorites having density of 2.67 g/cm^3 in the area, wide existences of these high density rocks at depth agree with A-district classified as high density area.

On the other hand, Mesozoic formations are widely distributed beneath younger volcanic rocks in B and C-districts. These formations have also rather higher density of 2.56 g/cm^3. Although this density is considered to be reasonable in B-district of intermediate density area, it is inconsistent with C-district where shows low Bouguer anomaly and is classified as low gravity area. B and C-districts are bordered by the most remarkable gravity lineament, which are presumed as major fault zones indicated by large gravity gradient. So that, it is suggested that considerable low density bodies are latent at rather shallow subsurface in C-district, and that a large-scale low gravity area may correspond to an extentive size of these bodies. In the investigation area of second phase survey, rocks and/or strata which are sufficient for such geological and physical conditions are not yet confirmed. Regarding this problem will be discussed again in the later paragraph 4.3.3. Interpretation on Low Gravity Anomaly in Eastern Area.

Next, local gravity anomalies obtained by relation between younger volcanic rocks and underlying basement rocks will be discussed. As is briefly mentioned before, areas distributing pumice tuff on the basement form locally small-scale low gravity anomalies. A-1 block and A-2 block in A-district are bordered by a remarkable gravimetric lineament of NE-SW system. The reasons why values of Bouguer anomaly at A-2 block are much lower than those at A-1 block can be interpreted to reflect remarkable differences of density between scoria tuff of 2.06 g/cm^3 at A-1 block and pumice tuff of 1.70 g/cm^3 at A-2 block. The same kind of pumice tuff is also distributed at A-3 block, and most of gravimetric synclinal structures are considered to be formed by structures of pumice tuff deposited locally in depressions of the basement.

In addition, gravimetric anticlinal and synclinal structures of NE-SW system are generally dominant in A-district. This fact indicates to repeat undulations elongating in NE-SW direction on paleotopography of the basement. In this connection, gravimetric lineaments in A-district are dominant in NE-SW system accompanied with those of N-S and E-W systems. They are the same lineaments as the remarkable lineament bordering B and C-districts and conjugate lineaments.

4.3.2 Structure of Gravity Basement based on Two-Dimensional Analysis

A-district, western parts of the investigation area, presents generally flat gravity distributions with lacking of variety. This means that paleotopographically, errosion surface of the basement was rather flat with a little uneveness.

According to calculated results on depth of gravity basement shown in Fig. 4-15, Fig. 4-16 and Fig. 4-17, values of 0.6 or 1.0 g/cm^3 as balances of density between scoria tuff or pumice tuff and basement rocks. Based on these calculated results, it can be pointed out that structures of paleo-surface of the basement are very gentle as shown in each profile, and that depth from the present surface to top of the basement does not exceed more than

700 m even though at the deepest (cf. B-B' profile).

On the other hand, as shown in profiles of A-A' and B-B', depths of gravity basement suddenly increase at eastern parts of the area. An average density of Mesozoic formations widely distributing at these parts is 2.56 g/cm^3, which gives only small balances of 0.11 g/cm^3 and 0.14 g/cm^3 against granodiorites and metamorphic rocks, respectively. Based on calculated results, the depth of gravity basement reaches up to 6,000 m from the surface in case of 0.20 g/cm^3, and is estimated as more than 10,000 m in case of 0.11 ~ 0.14 g/cm^3.

However, because it is very difficult geologically to consider that Mesozoic formations are thicker than 6,000 m, it is necessary to interpret more appropriate geologic structure.

4.3.3 Interpretation on Low Gravity Anomaly in Eastern Area

As is described before, gravity distributions do not agree with geological distributions on the surface at eastern parts of the investigation area. Namely, despite distributions of Bouguer anomaly strongly indicate existences of rock and/or strata of considerable low density, Mexozoic formations of relatively of high density are widely distributed on and near the surface.

In order to dissolve this problem, it is necessary to consider other geologic structures at depths; for instance, Mesozoic formations of very low density containing very much water in their fractures and/or large-scale another rock-body of very low density situating beneath Mesozoic formations. The former hypothesis seems to be unreasonable because of no such evidences based on geological survey and physical examinations in laboratory.

On the contrary, the later hypothesis seems to be more possible, although it is not proved enough both geologically and geophysically. Because, it is possible to presume that among constituent rocks of Domuyo Volcano Complex, intrusive rocks of relatively low density ranging from rhyolite-porphyry to granodiorite-porphyry may exist widely beneath Mesozoic formations. According to regional geological map of Fig. 2-2, intrusive rocks of Domuyo Volcano Complex are widely distributed at central areas of box-shaped dome structure centering around Domuyo anticlinal axis. And, values of Bouguer anomaly suddenly decrease toward central areas of the dome of upheaval block movement. Thus, it is presumed that density of intrusive rocks is considerably lower than that of Mesozoic formation, and that distributions of Bouguer anomaly at eastern parts of the area correspond to underground structure of western parts of the dome.

In the investigation area, granodiorite-porphyry to be considered a member of intrusive porphyry belonging to Domuyo Volcano Complex only forms small scale intrusive body at upstreams of Covunco River, and is found as rolling stones at two places. An average density of granodiorite-porphyry by measurements of four specimens gives 2.48 g/cm^3, and this value is a little lower than that of Mesozoic formations. In case of 0.2 g/cm^3 as a balance of densities of in upper and lower layers, depth of gravity basement reaches up to 6,000 m from the surface based on results of two-dimensional analysis. If it regards thickness of Mesozoic formations as more or less 1,000 m, a scale of the inferred intrusive bodies is approximately 5,000 m thick with considerable their expansions which exceed wider areas

than low gravity area shown in Fig. 4-14. Although geologically it is difficult to infer such large-scale intrusive bodies as Tertiary hypabyssal activity, results of gravity prospecting indicate one of the possibilities of above-mentioned underground structure.

Another interpretation regarding low gravity anomaly at eastern areas is as follows; It is considered that large-scale intrusive bodies of acidic porphyry may exist at depths, which are related to eruptions of dacitic and rhyolitic lava flows belonging to Domo volcanic rocks of the latest volcanism in the investigation area. This hypothesis has no essential difference between hypabyssal activities of Domuyo volcanism and Domo volcanism, although there are differences of geological ages between middle Miocene to early Pliocene of Domuyo Volcano and Pleistocene of Domo Volcano.

4.3.4 Investigation on Fracture System

As data to study fracture systems in the investigation area, the followings are available.

i) Faults and fracture systems based on regional geological data and results of geological survey.

ii) Fracture systems by lineament analysis based on geological interpretations of Landsat image and aerial photograph.

iii) Fracture systems based on gravimetric transition zones.

iv) Fracture systems inferred by distributions of geochemical anomalous areas

and,

v) Fracture systems inferred by distributions of geothermal manifestations such as hot springs and fumaroles.

Fracture systems on the basis of items i) to iii) related to geologic structure are summerized as follows.

(1) Fracture system of N-S direction

Fracture system of N-S direction can be universally observed as faults accompanied with regional fold structure and indicated by lineaments as well as joints developed in granodiorites of the basement. This fracture system are of large-scale in general and are dominant from older formations from younger volcanic rocks.

(2) Fracture system of E-W direction

Fracture system of E-W direction is mainly recognized by regional lineaments, joints in granodiorite and gravimetric lineaments, and is if lower intensity than other fracture sys-

tems. It is considered to be fracture system developed mainly in older formations.

(3) Fracture systems of NW-SE and NE-SW direction

Directions of these fracture systems range from NW-SE to WNW-ESE and from NE-SW to NNE-SSW. They can be peculiarly observed by faults, joints in granodiorite and gravimetric lineaments accompanied with gravimetric anticlinal and synclinal structures. It is considered to be fracture systems conjugating with large-scale fracture system of N-S direction.

Fracture system has important keys to reveal geothermal system, because the system participates in formations of geothermal fluid reservoir and in passages of ascending geothermal fluid. It can be said that locations of geothermal outcrops such as hot springs and fumaroles, distributions and conditions of hydrothermal alteration zones and geochemical anomalous areas of Hg-CO_2 concentrations, etc. are very faithful to feature systems. Especially, intersections of fracture system and fractures developed in the basement at depths close to heat source are tectonically the most important factor to develop geothermal energy.

Interpretations regarding fracture system in the investigation area are under stages of qualitative analysis based on results of present survey, and it is necessary to study in more detail by seismic prospecting of reflection method and test drilling.

4.4 Summary of Geologic Structure

(1) The investigation area is geotectonically divided into two areas. In western half, basement rocks consisting of metamorphic rocks and granodiorites exist at rather shallow parts from the surface, and younger vaolcanic rocks widely covers their flat paleotopographic surface. On the contrary, in eastern half, Mesozoic formations overlying on hidden basement rocks at depths are influenced by regional fold structure and local dome structure.

(2) Subsurface structure based on physical properties of constituent rocks forms two-layed structure. Namely, two-layered structure in western parts is composed of upper layer of younger volcanic rocks represented by low density and high effective porosity and of lower layer of basement rocks represented by high density and low effective porosity. On the other hand, two-layered structure in eastern parts is composed of upper layer of younger volcanic rocks and of lower layer of underlying Mesozoic formations represented by medium gravity and effective porosity, and basement rocks of high gravity and low effective porosity are latent at depths.

(3) Regarding regional gravity distributions, high Bouguer anomalous area corresponds to distributions of pre-Tertiary formations and low Bouguer anomalous area corresponds to distributions of Cenozoic volcanic rocks. It is a clear tendency to decrease values of Bouguer anomaly toward north, and the trend shows good correspondence of direction of fold structure and fault system.

(4) On the basis of distributions of Bouguer anomaly, the investigation area can be roughly divided into three districts; namely, A-district of high gravity area at west, C-district of low gravity area at east and B-district placed between A and C-district forming long and slender transition belt of N-S direction. Younger volcanic rocks of Quaternary age has no relevancy with general and regional gravity distributions, but only local relevancy is recognized between distribution of tuffs of low density and low gravity anomaly.

(5) A-district of high gravity area harmonizes with underground structure to exist basement rocks of high density at rather shallow subsurface. On the surface, Mesozoic formations of intermediate gravity are widely distributed in B and C-districts, and no consistence is recognized between intermediate density and Bouguer anomaly in transition zone of B-district. However, in C-district at east which is bordered from B-district by gravimetric lineaments having remarkable gravity gradient and presuming as major fault zone, low gravity area of Bouguer anomaly cannot interpretate its characteristic without presuming considerably extensive rocks and/or strata of low gravity in underground.

(6) Structure of gravity basement at west analized by two-dimensional method gives flat paleotopography of the basement and its depth of less than 700 m at the deepest part. On the other hand, depths of gravity basement at east suddenly increase and reach more than 6,000 m deep from the surface in case of calculations by a balance of densities of 0.2 g/cm^3.

(7) As one of the hypothesis for geological factor to form low gravity area at eastern parts of the investigation area, Mesozoic formations of very low density containing very much water in their fracture. However, no positive evidence is obtained geologically. Although it is proved enough at present, geologicic structure at east of the area is presumed that low density bodies of acidic porphyry to be considered a member of intrusive facies of Domuyo Volcano Complex exist beneath Mesozoic formations with considerable scale both horizontally and vertically.

(8) Fracture systems in the region and the investigation area are represented by those of N-S and E-W direction. N-S system is large-scale and is recognized universally from older formations to younger volcanic rocks, and E-W system is rather weak and mainly observed in older formations. Fracture systems of NW-SE and NE-SW direction are characteristically recognized by faults, gravimetric lineaments and joints in granodiorite, and conjugate with large-scale fracture system of N-S direction.

5. Heat Flow Structure in the Investigation Area

5. Heat Flow Structure in the Investigation Area

5.1 Alteration Zone

5.1.1 Purpose and Method of Alteration Survey

(1) Purpose

Aiming to clarify heat source bringing geothermal phenomena, form and scale of geothermal fluid reservoir, and geochemical characteristics of geothermal fluid, studies on temperature and circulation of geothermal hot water which brought hydrothermal alteration are carried out based on kinds, combinations and distributions of hydrothermal alteration minerals.

(2) Method

Keeping with geological survey, alteration survey was done, and locations and expansions of alteration zone, intensity of alteration and kinds of alteration minerals were plotted in route maps. Representative alteration zones showing some unities among all of them were surveyed their locations with topography by transit, compass and measuring tape, and distributions of alteration minerals and travertines are recorded in detail. Specimens taken from representative alteration zones were supplied for X-ray diffraction analysis.

Combined with detected alteration minerals by X-ray diffraction analysis and intensity of alteration observed in the field, zoning and genesis of alteration zones were interpreted.

5.1.2 Conditions of Each Alteration Zones

Fig. 5-1 shows locations of alteration zone, and Fig. 5-2 gives sketched areas of alteration zone and regional distributions of alteration minerals. Besides, details of each alteration zones are shown in Fig. 5-3 to Fig. 5-11, and intensity diagrams of each mineral based on X-ray diffraction method are presented in each figure. Index of each mineral is given in Fig. 5-3.

(1) Rincon de Las Papas (Fig. 5-3)

At Rincon de Las Papas, travertines are recognized in approximately 30 m by 30 m at two places near hot springs. Travertines are mostly composed of calcite, and rocks accompanying with travertines yield a very little quantity of kaoline. Geology of their vicinity mostly covered by talus deposits, soil and gravel consists of Chacay Melehue Formation, and alteration zone may expand in subsurface along or near boundary between the Formation and younger andesitic rocks.

(2) Arroyo Ailinco (Fig. 5-2)

Altered andesite to yellowish white-color crops out at both banks of downstreams of Ailinco River near confluence with Varvarco River. Despite no strong manifestation but only mineral springs, there is white-colored alteration zone which elongates in direction of N70° ~

80°E parallel to joint system in Quaternary andesite and assumed fault along Ailinco River. In this alteration zone, intensity of alteration ranges from strong argillic alteration spreaded in whole rock to weak and partial alteration only along joint system. Therefore, andesite appears fragile parts by argillization and megascopically fresh parts at 2 ~ 3 cm intervals. As alteration minerals, montmorillonite is common, and clinoptiloite, kaoline mineral and halloysite are detected.

(3) La Bramadora (Fig. 5-4)

At La Bramadora, only travertines and rolling stones contained montmorillonite are observed at surrounding areas of fumaroles, and no alteration zone crops out covering by talus and surface soil. Travertine is characterized by rich in quartz, presences of kaoline mineral and aragonite as carbonate mineral.

(4) El Humazo (Fig. 5-5, 5-6 and 5-7)

In El Humazo area, alteration zones in geothermal manifestation area at upstreams (Fig. 5-6) are distributed in an area of 100 m by 100 m where talus deposits cover main parts. Montmorillonite is common, and cristobalite and clinoptiolite are found at marginal parts.

In geothermal manifestation area at mountain slope near El Humazo (Fig. 5-7), storng alteration zone of white argillization is observed in an area of 200 m by 50 m without travertines. Alteration minerals consist mainly of sericite, kaoline and pyrite with accessary montmorillonite and mixed layer mineral.

In the biggest geothermal manifestation area of El Humazo (Fig. 5-5), travertines widely are distributed in an area of 500 m by 200 m and more than 50 m thick. No alteration zone crops out because of coverage by travertines, and only postash feldspar of alteration product from rocks in travertine is found.

(5) Las Olletas (Fig. 5-8)

Travertines are widely distributed of Las Olletas, and calcite, cristobalite, rhodochrosite

Small-scale alteration zones of approximately 200 m by 100 m are intermittently distributed along Covunco River. In an area 500 m long from the most upstreams to down stream,

(6) Los Tachos (Fig. 5-9, 5-10 and 5-11)

Small-scale alteration zones of approximately 200 m by 100 m are intermittently distribute along Covunco River. In an area 500 m long from the most upstreams to down stream, the strongest alteration zones converted into white-colored argillized zones are found consisting of crystobalite, kaoline mineral, montmorillonite and accessary halloysite, alunite, mixed layer mineral, sericite and olinoptiloite. In addition, there is no extensive alteration zone along down streams of Covunco River but only small-scale ones are observed near geothermal manifestations. From these zones, kaoline mineral, holloysite, montmorillonite chinoptiloite and crystobatite are detected.

Table 5-1 Results of investigation of alteration zones

Name		Characteristics	Place and size of alteration zone	Alteration zoning	Wall rock	Structural control
Lincon de Las Papas		(travertine)	The nearest area of the hot spring (30 m x 30 m)	- Kaolinite	Pyroclastics in Chacay Melehue F.	Boundary of Chacay Melehue formation and Quaternary volcanics
Arroyo Ailinco		decolorization	Along the Å Ailinco (about 700 m x 100 m)	Montmorillonite Kaolinite Haloysite	Quaternary andesite	Faults of ENE-WSW trend
La Bramadora		argillization	The neighborhood of the fumarole (20 m x 20 m)	Kaolinite (Cristobalite)	Quaternary dacitic pyroclastics	Faults of WNW-ESE trend
El Humazo	(2)	travertine	The neighborhood of the fumarole (accompanying float of white altered rock)	Kaolinite (Montmorillonite)	Quaternary andesite	Boundary of Chacay Melehue formation and young dacite
	(3)	argillization	same as above (smaller than 200 m x 50 m)	Kaolinite (Montmorillonite)	Quaternary dacite	
	(1)	green argillization	Thickness: more than 50 m accompanying greenly argillized boulder	- (Potash feldspar)	Chacay Melehue F.	
Las Olletas		travertine	500 m x 200 m	- (cristobalite)	Granodiorite	Boundary of granodiorite and young andesite
		decolorization	neighborhood of travertine			
Aguas Calientes		travertine	The neighborhood of hot springs along Å Agua Calientes	-	Quaternary andesite Scoria tuff	Joints in scoria tuff
Baños del Aguas Calientes		travertine	Along Å Banos del Agua Caliente (smaller than 30 m x 30 m)	-	Quaternary andesite	Joints in scoria tuff
Los Tachos	(3)	argillization	Along Å Covunco (smaller than 200 m x 100 m)	Cristobalite caolinite Montmorillonite	Quaternary dacite	Faults of E-W trend
	(2)	argillization	same as above		Dacitic pyroclastics	
	(1)	(partly argillized)	same as above		Quaternary dacite	

Table 5-2 List of alteration minerals

Group		Name of alteration mineral	Chemical composition	Estimated condition of occurrence				
				Temperature °C			pH	
				∿ 100	100 ∿200	200 ∿	acidic	neutral alkaline
Silica minerals		Opal	$SiO_2.nH_2O$	o			o	o
		Cristobalite	SiO_2	o			o	o
		Tridymite	SiO_2	o			o	
		Quartz	SiO_2		o	o	o	o
Zeolites		Clinoptiloite	$(Na, K, Ca)_{15}[Al_{1.5}Si_{7.5}O_{18}]5H_2O$	o				o
		Heulandite	$Ca[Al_2Si_7O_{18}].6H_2O$	o	o			o
Clay minerals	Smectite	Montmorillonite	$(Al.Mg)_2[(OH)_2](Si,Al)_4O_{10}]Na_{0.33}.4H_2O$	o				o
	Kaoline	Halloysite	$Al_4[(OH)_8]Si_4O_{10}].4H_2O$	o			o	
		Kaolinite	$Al_4[(OH)_8]Si_4O_{10}]$	o	o		o	
	Mica	"Sericite"	$KAl_2[(OH_2](Si,Al)_4O_{10}]$		o	o	o	o
	Chlorite	"Chlorite"	$(Al,Fe,Mg)_3[(OH)_2](Si,Al)_4O_{10}].(Al,Mg,Fe)_3(OH)_6$		o	o		o
	Mixed layer type	Sericite/ Montmorillonite	$K(Al,Mg)_4[(OH_4)](Si,Al)_8O_{20}]Na_{0.33}.4H_2O$	o	o		o	o
Others		"Potassium feldspar"	$K[AlSi_3O_8]$			o		o
Sulphate		Alunite	$KAl_3[(OH)_6(SO_4)_2]$	o	o	o	o	
		Gypsum	$Ca[SO_4].2H_2O$	o	o	o	o	o
		Anhydrite	$Ca[SO_4]$	o	o	o	o	o

5.1.3 Zoning of Alteration Zones

Table A-7 in appendix presents whole results of X-ray diffraction analysis, and Fig. 5-12 shows representative charts of the analysis. These results are summarized in Table 5-1, and characteristics of alteration minerals detected in the area are given in Table 5-2.

(1) Classification of alteration zoning and its character

Minerals formed through process of geothermal alteration are various. Based on combinations of alteration mineral to be considered primary products of geothermal alteration, zoning of alteration zones can be established dividing into eight zones; namely, 1) crystobalite zone, 2) halloisite zone, 3) kaoline zone, 4) montmorillonite zone, 5) alunite zone, 6) mixed layer mineral zone, 7) sericite zone and 8) heulandite zone. Among them, later four ones of 5) to 8) are intermittent in their distributions. Besides, alteration zones in the area are distributed separating each other, and non-alteration zones are located between each alteration zones. In general, they are rather small-scale except relatively wide alteration zone at upstreams of Los Tachos.

Accordingly, because areas of alteration zone which are possible to show their zonings in figure are limited, zoning of alteration zone at Los Tachos-3 is shown in Fig. 5-13 as an example. Zoning of alteration zones given in Table 5-1 is divided into 1) crystobalite zone, 2) halloisite zone, 3) kaolinite zone and 4) montmorillonite zone, which zoning is based on temperature and characteristics of hot water anc fumarolic gas.

1) Crystobalite zone

α-crystobalite is generally formed by silicification. Although it much easily proceeds under acidic condition of low temperature, even intermediate or alkaline conditions are suitable for its formation. Crystobalite zone settled hereby is defined as zone consisting mainly of α-crystobalite accompanying with trydemite and clinoptiloite, but without montmorillonite, kaoline and halloysite.

In case this alteration is remarkable, α-crystobalite appears independently or as main constituent mineral. However, it is characterized by a kind of the weakest geothermal alteration which volcanic glass is converted into α-crystobalite, and by its wide distribution around other alteration zones.

2) Halloisite zone

Halloisite alteration indicates acidic condition of low temperature. This alteration zone is established because of one of geothermal alterations in the area, although halloisite may appear as product of weathering. In this zone, crystobalite, trydemite, amorphous silica mineral and montmorillonite are associated. In case of paragenesis with montmorillonite, it is possible to set its alteration zone into montmorillonite zone or to establish subzone as overlaped alteration zone.

3) Kaoline zone

Kaoline alteration is formed under acidic condition of low to intermediate temperature which is relatively higher than that of halloisite alteration. This zone is characterized by kaoline mineral and is occasionally accompanied with montmorillonite, alunite, heulandite, crystobalite, amorphous silica mineral, pyrite and a little quality of mixed layer mineral, chlorite and sericite.

4) Montmorillonite

Montmorillonite alteration indicates intermediate to alkaline condition of low to intermediate temperature. Although this is defined alteration zone consisting mainly of montmorillonite without halloisite and kaoline, clinoptiloite, crystobalite, trydemite, mixed layer mineral, chlorite and sericite are occasionally accompanied.

(2) Characteristics of alteration zoning of the investigation area

Based on establishment of above-mentioned alteration zoning, alteration zones of geothermal manifestation in the area are characterized as follows; Namely crystobalite zone, kaoline zone and montmorillonite zone are closely connected with each other in each alteration zones, and generally form zoning of kaoline zone at core surrounding fumaroles, montmorillonite zone at the intermediate and crystobalite at shell.

As show in Fig. 5-13, alteration zones at Los Tachos elongate parallel to Covunco River, and form zoning of inner kaoline zone and outer crystobalite zone, Montmorillonite zone is considered to be the middle surrounding kaoline zone, but it might be possible to interpretate that montmorillonite zone cuts kaoline zone.

As a result of observations in the field, alteration zoning in each geothermal manifestation areas have been independently formed a sequence of hydrothermal alterations, because there are non-altered zones between each alteration zones. However, taking a general view of characteristics of alteration zone in the whole area, kaoline alteration zone indicating acitic condition of low to intermediate temperature more widely occupies in eastern areas such as La Bramadora, mountain slope of F1 Humazo and uptreams of Los Tachos, and montmorillonite indicating intermediate to alkaline condition of low temperature is dominant in western areas. In addition, alteration zone at La Bramadora is accompanied with alunite which is formed under acidic condition of low to high temperature.

5.1.4 Considerations on Hydrothermal and Solfataric Alterations as Geothermal Manifestations

Zonal distribution of hydrothermal alteration in each geothermal manifestation areas and relatively regional zonings taken a general view in the whole areas give one of the keys to several conditions of hydrothermal solution such as its temperature and pH which has been bringing geothermal phenomena.

Geothermal phenomena of young volcanic activity is roughly divided into vapor dominated system and water dominated system. There is a general tendency that the former

makes alteration zone consisting mainly of kaoline with accessary pyrite and cinnabar, and the later forms alteration zones of various type, depending on differences of pH condition, such as silica minerals, calcite, zealite and clay minerals. Besides, they say that water dominated system may convert into vapor dominated type because of intersections of supplying passage of geothermal hot water by depositions of alteration mineral.

From these points of view, alteration zones in the investigation area are considered as follows; Namely, alteration zones at La Bramadora, El Humazo and Los Tachos in eastern parts of the area are characterized by kaoline alteration which may be originated from vapor dominated system or water·vapor mixed system. And, thick travertines at El Humazo or silica minerals in rolling stones distributing in areas from El Humazo to Los Tachos may suggest that water dominated system had formerly existed in these areas. Travertines at El Humazo have been deposited up to 50 m higher place than river bottom where hot springs and fumaroles exist at present. Therefore, these travertines are not originated from present hot water, but made by past one.

On the contrary, alteration zones in western parts of the area are considered to be formed by geothermal phenomena of water dominated system, and are mainly composed of montmorillonite with accessary zeolite and silica minerals. Travertines widely distributed at Las Olletas have been deposited present hot water which is running on the surface of travertines. Although they are small-scale, the same type of travertines are observed at Rincon de Las Papas and Aguas Calientes, etc.

As a result of studies on hydrothermal alteration zones and travertines in the investigation area, it is considered that geothermal systems gradually change from vapor dominated system indicated by acidic condition of low to intermediate temperature to water dominated system indicated by intermediate to alkaline condition of low temperature with overlapped acidic condition of low temperature, in proportion as areas from La Bramadora at east to Banos del Agua Caliente at west.

5.2 Ground Temperature and Geochemistry

5.2.1 Purpose and Method of Ground Temperature Survey at 1 Meter Depth and Geochemical Prospecting

(1) Purpose

Distributions and forms of anomalous area of ground temperature in the geothermal field directly give data regarding heat flow structure related to location, form and/or intensity of heat source at depths. Aiming to obtain informations of underground heat flow structure and to contribute to decide locations of test holes at 100 m depth for measurement of ground temperature in the third phase survey, ground temperature survey at 1 m depth was carried out during the second phase survey.

On the other hand, geochemical surveys of Hg and CO_2 concentrations by studies on distributions of contents of Hg-vapor and CO_2-gas ascending from depths through fractures were conducted, intending to interpretate structure of fracture system hidden in underground

and to obtain data on an activity of geothermal system.

Because these three methods are done at the same time and the same measuring points, informations on heat flow structure are expected at high accuracy by their combinations.

(2) Method

Square grid at 500 m was set in the area, and total 460 measuring points located in each grids had been scheduled. Besides, additional 57 points were measured in remarkable geothermal manifestation areas at central parts of the area. Fig. 5-14 shows location of measuring points.

Ground temperature survey was done by drilling test holes of one meter deep to be able to ignore diurnal variation, and by measurement by thermister thermometer. Distribution survey of Hg-concentration is to detect contents of Hg-vapor which ascends from the depth to the surface and is absorbed in soil. Soil samples taken from bottom of each test holes at 1 m depth were supplied to chemical analysis, and Hg-gas densities are obtained in unit of ppb. Distribution survey of CO_2-concentration is to measure contents of CO_2-gas which ascends as volcanic gas or soluble gas in hot water and concentrates in soil-air. Because it can be easily measured by gas chromatometer, CO_2-gas densities in soil-air in each test holes at 1 m depth are obtained in unit of %.

5.2.2 Measurement and Analysis of Ground Temperature at 1 Meter Depth

(1) Results of ground temperature measurement

Fig. 5-15 shows results of ground temperature measurements, and Table 5-3 and Fig. 5-16 give statistical values and frequency distribution of ground temperature at 1 m depth, respectively.

Measured values range from 5.8°C to 57.0°C with an average of 14.3°C. Low temperature area of approximately 10°C including minimum of 5.8°C occupies areas of high elevation at east, and high temperature area of more than 18°C including maximum of 57.0°C are located in and near geothermal manifestations such as El Humazo, Los Tachos, Las Olleta and Aguas Calientes, and at southwestern parts of the area. Fig. 5-19 shows distribution of ground temperature at 1 m depth by running average method, which is drawn contour lines by arithmetic averages of measured values in each circles of a radius of 1 Km, in order to find a tendency of their distributions smoothed by removal of local anomalies shown in Fig. 5-15.

(2) Fixed point observation

Atmospheric temperature and ground temperature were observed at fixed point settled at 200 m northwest of the Base camps. Fig. 5-17 shows results of these observations recorded each one hour during periods from 8 a.m. to 8 p.m. of Jan. 18. Although variations of atmospheric temperature range 10°C during half a day, ground temperature at 1 m depth changes only 0.3°C. Besides, Fig. 5-18 shows observational results of variation of atmospheric and ground temperatures during periods of 1 m depth survey, and variations of the later at the fixed point were limited to 0.7°C.

Table 5-3 Frequency distribution of temperature at 1 m depth

Range No.	Range	Frequency	Cumulative frequency
1	57.00000 - 53.58670	1 (0.20%)	1 (0.20%)
2	53.58670 - 50.17330	0 (0.00%)	1 (0.20%)
3	50.17330 - 46.76000	0 (0.00%)	1 (0.20%)
4	46.76000 - 43.34670	0 (0.00%)	1 (0.20%)
5	43.34670 - 39.93330	0 (0.00%)	1 (0.20%)
6	39.93330 - 36.52000	2 (0.40%)	3 (0.60%)
7	36.52000 - 33.10670	1 (0.20%)	4 (0.80%)
8	33.10670 - 29.69330	1 (0.20%)	5 (1.00%)
9	29.69330 - 26.28000	1 (0.20%)	6 (1.20%)
10	26.28000 - 22.86670	4 (0.80%)	10 (2.00%)
11	22.86670 - 19.45330	15 (2.99%)	25 (4.99%)
12	19.45330 - 16.04000	107 (21.36%)	132 (26.35%)
13	16.04000 - 12.62670	190 (37.92%)	322 (64.27%)
14	12.62670 - 9.21333	146 (29.14%)	468 (93.41%)
15	9.21333 - 5.79999	33 (6.59%)	501 (100.00%)

Number	501						
Maximum	57	Average (M)	14.287		Minimum	5.8	
Standard deviation	(σ)	4.18607	M + σ	18.4731	M + 2σ		22.6592

Table 5-4 Frequency distribution of Hg - concentration

Range No.	Range	Frequency	Cumulative frequency
1	2308.30000 - 1345.07000	2 (0.40%)	2 (0.40%)
2	1345.07000 - 783.79000	0 (0.00%)	2 (0.40%)
3	783.79000 - 456.72400	0 (0.00%)	2 (0.40%)
4	456.72400 - 266.13800	3 (0.60%)	5 (1.00%)
5	266.13800 - 155.08200	4 (0.80%)	9 (1.79%)
6	155.08200 - 90.36810	1 (0.20%)	10 (1.99%)
7	90.36810 - 52.65850	9 (1.79%)	19 (3.78%)
8	52.65850 - 30.68470	20 (3.98%)	39 (7.77%)
9	30.68470 - 17.88040	64 (12.75%)	103 (20.52%)
10	17.88040 - 10.41910	133 (26.49%)	236 (47.01%)
11	10.41910 - 6.07133	175 (34.86%)	411 (81.87%)
12	6.07133 - 3.53783	61 (12.15%)	472 (94.02%)
13	3.53783 - 2.06154	20 (3.98%)	492 (98.01%)
14	2.06154 - 1.20128	9 (1.79%)	501 (99.80%)
15	1.20128 - 0.70000	1 (0.20%)	502 (100.00%)

Number	502						
Maximum	2308.3	Average (M)	10.95		Minimum	.7	
Standard deviation	(σ)	.371326	M + σ	25.7477	M + 2σ	60.5431	

(3) Altitude correction and data processing

Altitude correction of measured ground temperatures are required, because elevations of measuring points range from 1,500 m to 3,500 m, and these balances have an effect on ground temperature. According to Fig. 5-20, influences of elevation can be clearly recognized in which distributions of ground temperature are in inverse proportion to topographic heights. This tendency is also shown by contour lines in Fig. 5-19.

Because coefficient of correlation between elevation and ground temperature at each measuring points is given as $\gamma = -0.74$ which means statistically capable, relations of both values are approximately given by the following equations.

linear equation. $T = 26.91 - 5.910 \times 10^{-3}H$ ..... (1)

quadratic equation: $T = 35.61 - 0.01376H + 1.717 \times 10^{-6}H^2$ ..... (2)

T: temperature (°C)

H: elevation (m)

A value of ΔT, a balance of temperature at each measuring points which is subtracted T°C calculated by above equations from measured temperature at 1 m depth, is called residual ground temperature. Fig. 5-21 and Fig. 5-22 show contour lines of residual ground temperature.

(4) Analytical results

Distribution maps of residual ground temperature are made after data processing of altitude correction. Both cases calculated by two equations have a nearly same tendency as shown in Fig. 5-21 and Fig. 5-22.

Compared these maps of residual ground temperature with contour line map of measured ground temperature, areas of geothermal manifestation such as El Humazo, Los Tachos, Las Olletas and Aguas Calientes, where high ground temperatures more than 18°C were measured, are confirmed as ground temperature anomalous area having more than 5°C of residual ground temperature. In addition to these anomalous areas, the same kinds of anomalies are recognized at downstreams of Banos del Agua Coliente in southeastern parts and at northeastern corner of the investigation area.

5.2.3 Survey and Analysis of Distributions of Hg-Concentration in Soil

(1) Results of Hg-concentration survey

Fig. 5-23 shows distributions of Hg-concentration, and Table 5-4 and Fig. 5-24 give statistical values and frequency distribution of Hg-concentration, respectively.

Values of Hg-concentration widely range 0.7 to 2,308 ppb with an average value of 11 ppb, and a value of average M plus a value of standard deviation σ is 26 ppb. On the basis of this value of $M + \sigma$ as threshold value, high anomalous areas of Hg-concentration are extracted at and near Cerro de La Papa, El Humazo, Los Tachos and Aguas Caliente.

(2) Analytical results

Fig. 5-25 shows contour line map made by running average method in order to search

a tendency of the whole area smoothed by removal of local anomalies.

Anomalous areas at northeast including measured point of maximum 176.6 ppb concentrate in an area of 2 Km along creek trending NNW direction. Anomalous areas surrounding El Humazo are widely distributed from western limit of fumaroles at downstreams to hilly regions at east, and have a maximum value of 417.2 ppb. Anomalous areas at Los Tachos elongate in E-W direction along Covunco River, and its extension reaches approximately 7.5 Km where three low value areas are located at the middles.

These three anomalous areas of Hg-concentration are emphasized in Fig. 5-25, and are major anomalies trending in NNE-SSW direction.

Anomalous areas near Aguas Calientes are located along drainage system of ENE-WSW direction, and small-scale anomalous areas at downstreams of Manchana Covunco River and at southeast of Las Olletas are locally recognized.

5.2.4 Survey and Analysis of Distributions of CO_2-Concentration in Soil-Air

(1) Results of CO_2-concentration survey

Fig. 5-26 shows distributions of CO_2-concentration, and Table 5-5 and Fig. 5-27 give statistical values and frequency distribution of CO_2-concentration, respectively.

Values of CO_2-concentration range from 0.03 to 2.6% with an average value of 0.1%, which are rather low values of CO_2-concentration than usual values in geothermal fields. On the basis of threshold value of 0.18% calculated by average value M + standard deviation σ, anomalous areas of relatively small-scale distribute are scattered at or near areas of geothermal manifestation, as shown in Fig. 5-26.

(2) Analytical results

Fig. 5-28 shows contour line map made by running average method. As a result of analysis based on this map, three remarkable anomalous areas are obtained at Cerro de La Papa and its south, Los Tachos and north of the Base camps. Otherwise, small-scale anomalous areas scattered at and near other areas of geothermal manifestation are mostly disappeared.

Thus, although generally small-scale anomalous areas of CO_2-concentration are recognized at each places in the investigation area, an anomalous area directly corresponding with present geothermal manifestation is only that of Los Tachos.

5.2.5 Considerations on Anomalous Areas of Ground Temperature and Hg-CO_2 Concentration as Geothermal Manifestations

(1) Correlation between ground temperature, and Hg-concentration and CO_2-concentration

Regarding correlation between ground temperature, and Hg and CO_2-concentrations at each measuring points, coefficients of correlation each other are statistically very small values. Although coefficient of correlation between residual ground temperature and Hg-concentrate gives $\gamma = 0.34$ showing low correlation, almost nothing is found between residual

Table 5-5 Frequency distribution of CO_2 gas-concentration

Range No.	Range	Frequency	Cumulative frequency
1	2.60000 - 1.93100	3 (0.60%)	3 (0.60%)
2	1.93100 - 1.43415	0 (0.00%)	3 (0.60%)
3	1.43415 - 1.06513	0 (0.00%)	3 (0.60%)
4	1.06513 - 0.79107	2 (0.40%)	5 (1.00%)
5	0.79107 - 0.58752	5 (1.00%)	10 (2.00%)
6	0.58752 - 0.43635	0 (0.00%)	10 (2.00%)
7	0.43635 - 0.32407	4 (0.80%)	14 (2.79%)
8	0.32407 - 0.24069	10 (2.00%)	24 (4.79%)
9	0.24069 - 0.17876	26 (5.19%)	50 (9.98%)
10	0.17876 - 0.13276	55 (10.98%)	105 (20.96%)
11	0.13276 - 0.09860	176 (35.13%)	281 (56.09%)
12	0.09860 - 0.07323	72 (14.37%)	353 (70.46%)
13	0.07323 - 0.05439	64 (12.77%)	417 (83.23%)
14	0.05439 - 0.04039	42 (8.38%)	459 (91.62%)
15	0.04039 - 0.03000	42 (8.38%)	501 (100.00%)

Number	501				
Maximum	2.6	Average (M)	.0960153	Minimum	.03
Standard deviation	(σ) .264496	M + σ	.176537	M + 2σ	.324588

ground temperature and CO_2-concentration.

Next, as a result of studies on mutual relations of measured values of ground temperature, Hg-concentration and CO_2-concentration at each measuring points, anomalous values of three methods overlapped at the same point are only three measuring points which are one at southeast of El Humazo and two at Los Tachos. Two of anomalous values from three method overlapped at the same point are ten measuring points. Although they generally show a bad unity, seven measuring points among ten are distributed in areas of geothermal manifestation such as El Humazo, Las Olletas and Arroyo Aguas Calientes.

(2) Mutual relation between anomalous areas of ground temperature and geochemistry

As is mentioned the above, no satisfied results are obtained by mutual relations between anomalous values of ground temperature and geochemistry at each measuring points. Accordingly, study on mutual relations between anomalous areas obtained by three methods was conducted as shown in Fig. 5-32, based on combinations of residual ground temperature of Fig. 5-21, Hg-concentration of Fig. 5-23 and Fig. 5-25, and CO_2-concentration of Fig. 5-26 and Fig. 5-28.

It can be said that anomalous areas by residual ground temperature generally correspond well to areas of geothermal manifestation. Namely, in western half of the area, a group of anomalous areas from Las Olletas through Arroyo Aguas Calientes to its southwest stands a line trending in ENE-WSW direction. And, an anomalous area at western margins of Los Tachos elongate in direction of NE-SW, and is accompanied with satellite anomalous areas at its northwestern side. At its northeastern extension, an anomalous area of south of El Humazo is located connecting to semi-anomalous area of Cerro de La Papa in direction of NNE-SSW. On the other hand, no anomalous area of ground temperature is found in areas of geothermal manifestation at Rincon de Las Papas and Arroyo Ailinco.

Mutual relations between these anomalous areas of ground temperature and anomalous areas of Hg-concentration are summarized as follows; namely, anomalous areas of Hg-concentration corresponding to those of ground temperature at Las Olletas, Aguas Calientes and its southwest is only limited to rather small-scale anomalous area which turns to semi-anomaly of Hg-concentration by running average method. On the contrary, three anomalous areas of Hg-concentration, sub-axis elongating in N-S or NW-SE direction can be recognized.

Next, mutual relations between anomalous areas of ground temperature and those of CO_2-concentration are sammarized as follows; namely, although both anomalous areas are well identical with each other at Los Tachos, other anomalous areas of CO_2-concentration scatter surrounding areas of anomalies of ground temperature without good correspondences. However several anomalous areas of CO_2-concentration, standing a line of NNE-SSW direction at areas from Los Tachos through its southeast and southeast of El Humazo to Cerro de La Papa, stand a line corresponding with above-mentioned trends of both anomalous areas of ground temperature and Hg-concentration. More remarkable trend of anomalous areas of CO_2-concentration is a sequence of several anomalous areas in NW-SE direction located from Arroyo Ailinco to southeast of El Humazo, as well as a sequence of anomalous areas parallel

to the above trend located from middle streams of Varvarco River through north of the base camps, southeast of Las Olletas and north of Los Tachos to eastern margin of Los Tachos.

Anomalous areas obtained by running average method, are concentrated in three areas of Los Tachos, east of Cerro de La Papa and north of the base camps.

Finally, regarding mutual relations between anomalous areas of Hg and CO_2 concentrations, both anomalous areas are approximately identical at Los Tachos, and show some relations at southeast of El Humazo. However they are generally distributed independently or separately.

Thus, degrees of their mutual relations have a tendency to decrease in the following order; namely, 1) areas of geothermal manifestation and those of ground temperature anomaly, 2) anomalous areas of ground temperature and Hg-concentration, 3) anomalous areas of ground temperature and CO_2-concentration, as well as those of Hg and CO_2-concentrations.

(3) Relation between ground temperature – geochemistry anomaly and heat flow structure – fracture system

Heat from heat source or geothermal fluid reservoir of high temperature at depths is conveyed to or near the surface by manners of thermal conduction of rocks and/or thermal transportation through heat transfer media of geothermal fluid such as geothermal hot water, stream and gas. Almost all of anomalous areas of ground temperature obtained by the second phase survey can be connected with areas of geothermal manifestation of hot springs and/or fumaroles. It is interpretated that these anomalies are mainly caused by thermal transportations, and geothermal fluid has been ascending through fracture system of NE-SW direction as its passage from depths indicated by trends of hot springs, fumaroles and ground temperature anomalies. It is expected, through heat flow survey by 100 meters deep test holes planed as the third phase survey, to reveal more detailed characteristics of ground temperature anomaly originated from combinations of thermal conduction and thermal transportation.

Anomalous areas of Hg-concentration have been formed by ascents of Hg-vapor from depths through fracture system, absorption in soil and concentration. Therefore, it is common that Hg-vapor more easily ascends in vapor dominated system of geothermal system than water dominated system, and that much higher values of Hg-concentration are expected in case of less hot water. Based on distributions and intensities of Hg-concentration in the investigation area, it is suggested that eastern parts of the area show higher geothermal activities than western parts. In addition, main fracture systems in direction of NE-SW including ENE-WSW and NNE-SSW together with secondary fracture systems in direction of NW-SE, N-S and E-W are proved trends of anomalous areas of Hg-concentration.

Anomalous areas of CO_2-concentration have been formed by concentrations in soil-air ascending from depths as free or soluble CO_2-gas in hot water. In general, CO_2-concentration in the investigation area is lower than that of other geothermal fields. Anomalous areas of CO_2-concentration in western parts, where amounts of hot water are much more compared with eastern parts and are represented by hot springs without fumaroles at Aguas Calientes,

are considered as results of separation of CO_2-gas from soluble gas in hot water near the surface. On the contrary, anomalous areas distributed from Los Tachos to southeast of El Humazo are probably caused by much free CO_2-gas, because there are relationships with ground temperature and Hg-concentration anomalies accompanying with fumarolic gas. As is mentioned before, fracture system of NE-SW is recognized at A-district in western parts are recognized by gravity anomaly as gravimetric anticlinal and synclinal structures. In addition to this, another important fracture system of NW-SE direction in this area is proved by two parallel arrangements of anomalous areas of CO_2-concentration.

5.3 Heat Source

5.3.1 Volcanic Activity

Volcanic activities of post-Paleogene Tertiary in the region and investigation area took place twice; namely, they are Domuyo volcanism during periods from middle Miocene to early Pliocene, and intermediate volcanism occurred during periods from and of Pliocene to earlier half of Pleistocene and continued on into acidic Domo volcanism in later half of Pleistocene.

In general, it is said that a life of magmatic activity brought single volcanism is several ten thousands or maximum hundred to two hundreds thousands years. However, in case of large-scale and composite volcanism like Domuyo Volcano, it seems to be reasonable to consider much longer life of magmatic activities, even though each unit magmatism of them had rise and fall. If it is premised that volcanism of Domuyo Volcano was extinct at early Pliocene time, its age is four to five million years ago and magma reservoirs of Domuyo Volcano were already disappeared. Therefore, it is unreasonable to consider these magmatic activities as heat source which has brought present geothermal phenomena.

Accordingly, heat saurce bringing present geothermal system should be searched for magma reservoir accompanied with activities of Domo Volcano which took place at much younger age of later half of Pleistocene time. As is mentioned before, absolute ages of lava flows belonging to Domo volcanic rocks are determined 0.72 ± 0.10 Ma as the oldest and 0.11 ± 0.02 Ma as the youngest together with other ages of the middle. That is, Domo volcanism is interpretated as a sequence of acidic volcanism ranging from dacite to rhyolite taken place during periods from middle of early Quaternary to end of Quaternary, even though each unit magma reservoirs may have been repeated ups and downs.

At present, it is not entirely clarified the whole characteristics such as types and centers of volcanism regarding younger volcanos including Domo Volcano. Based on Regional geological map shown in Fig. 2-2 and Geological interpretation map of serial photo shown in Fig. 2-3, however, it is assumed that younger volcanism has two or three centers of volcano in areas five to ten kilometers southeast of the investigation area together with another center of volcano at or near La Bramadora area in the investigation area. Thus, younger volcanism in Quaternary age is characterized by composite volcanos having several centers of activity. At present, active geothermal manifestations are recognized and limited in the area from La

Bramadora to its west where one of the centers of volcanism is assumed. This fact seems to indicate relations between the youngest volcanism and present geothermal phenomena.

5.3.2 Magma Reservoir as Heat Source

It is inferred that magma reservoir as origin of volcanism is situated at several to ten kilometers deep from the surface, and has a scale of several kilometers in diameter and temperatures of 700°C to 1,000°C. Magma from its reservoir erupts intermittently and forms volcanos. Magma consists mainly of fluidal silicates originated from melting of rocks, and is accompanied with gas, steam and magmatic water.

Although it is difficult to make clear entirely regarding depth, location, scale and temperature of magma reservoir in this region, based on present data obtained, it is assumed that heat source locates at and near La Bramadora area in eastern parts of the investigation area, and expands at depths of the area.

5.4 Summary of Heat Flow Structure

(1) Hydrothermal alteration zones and travertines are observed at areas of geothermal manifestation such as hot springs and fumaroles. Alteration zones are divided into 1) crystobalite zone, 2) holloysite zone, 3) kaoline zone and 4) montmorillonite zone. They generally show zoning of alteration having a tendency of kaoline zone in core, montmorillonite zone in middle and crystobalite in shell.

(2) Taking a general view of alteration zoning in the whole area, characteristics of geothermal system is summarized as follows; namely, alteration zones at La Bramadora, El Humazo and Los Tachos in eastern parts of the area are characterized by kaoline alteration with alunite alteration under acidic condition of low to high temperature, which is originated from vapor dominated system or water-vapor mixed system. On the contrary, alteration zones in western parts of the area are considered to be gradually changed into montmorillonite zone under intermediate to alkaline condition of low temperature together with overlapped crystobalite zone under acidic condition of low temperature, which is caused by water dominated system.

(3) As a result of ground temperature survey at 1 m depth, anomalous areas of residual ground temperature calculated by altitude correlation trend on a line of NE-SW direction connected with geothermal manifestation areas in central-western and central-eastern parts. However, no anomalous area is found in northern geothermal manifestation areas.

Anormalous areas of Hg-concentration in central-eastern parts show good correspondence with those of ground temperature trending in NE-SW direction, and only small-scale semi-anomalous areas exist in central-western parts.

Although anomalous areas of CO_2-concentration at El Humazo are identical with those of ground temperature and Hg-concentration trending in NE-SW direction areas. The most characteristical trend of CO_2-concentration anomalies is shown by two parallel arrangements

in NW-SE direction elongating from northwest to southeast in the investigation area.

(4) Fracture systems and grades of geothermal activity in the area, based on anomalous areas of ground temperature and Hg-CO_2 geochemistry, are summarized as follows; namely, central-eastern parts are mainly characterized by anomalous areas of ground temperature and Hg-concentration accompanied with fracture systems in NE-SW direction, and grades of geothermal activity is higher than those in western parts. On the contrary, although anomalous areas of CO_2-concentration in western parts of the area which mainly prove fracture systems in NW-SE direction, grades of geothermal activity is rather low. In addition, there are fracture system of N-S and E-W direction indicated by Hg-CO_2 geochemical anomalies.

(5) Heat source bringing present geothermal phenomena in the area is considered to be magma reservoir which is related to younger volcanism of Quaternary age including Domo Volcano taken place during periods from 700 to 100 thousands years ago. One of the centers of volcanism is inferred to exist at depths of La Bramadora area, and heat source expands widely in subsurface of the area.